UNIVERSITÀ DEGLI STUDI DELL'AQUILA
DIPARTIMENTO DI SCIENZE CLINICHE APPLICATE E BIOTECNOLOGICHE

Dottorato di Ricerca in Medicina sperimentale

Curriculum Biotecnologie Mediche

XXXIII ciclo

Titolo della tesi

ULTRASOUND-BASED METHOD FOR IDENTIFICATION OF NOVEL MicroRNA BIOMARKERS IN PROSTATE CANCER

SSD MED/46

Dottoranda

Jessica Cornice

Coordinatore del corso

Prof. Mariagrazia Perilli

Tutor

Prof. Francesca Zazzeroni

A.A. 2019/2020

INDEX

ABSTRACT

Detection of circulating microRNA-based biomarkers represent an innovative, non-invasive, method for early detection of cancer. However, low concentration of miRNAs released in blood, especially in the early-stage disease, and difficult localization of the tumor site limited their clinical use as effective cancer biomarkers. The amplification of circulating cancer biomarkers mediated by ultrasound can potentially overcome these issues, thus advancing the use miRNA-base biomarkers in clinical setting. This work investigated the potential of an innovative ultrasound-based prototype to improve the release of miRNAs in the extracellular fluids, with the aim of identifying novel miRNA-based biomarkers to be used for prostate cancer diagnosis, as well as for monitoring disease evolution. We provided evidence that US-mediated sonoporation amplify the release of miRNAs from both androgen-dependent and – independent PCa cells, allowing the detection of novel miRNA with potential predictive and prognostic value. Moreover, we showed that ultrasound treatment improves drug delivery opening the route to new possible therapeutic applications.

KEYWORDS: miRNAs, Biomarkers, Prostate Cancer, Ultrasounds.

INTRODUCTION

PROSTATE CANCER EPIDEMIOLOGY AND RISK FACTORS

Prostate cancer (PCa) is a highly heterogeneous disease, representing the most common cancer with an important impact on men's health. One of the most challenging aspect of prostate cancer is the timing of diagnosis, since the advanced disease is often detected after screening or when the metastatic disease is already established (Chow et al., 1998). Moreover, the wide range of differences in PCa disease evolution - from hyperplasia to lethal castration resistant PCa (CRPC) - remains a major problem (Bonaccorsi et al., 2015).

Most types of PCa are known for their indolent and non-invasive nature, as well as for their strict association with age rather than other factors: 50% of men at the age of 50 and 80% at the age of 80 have it (Popa et al., n.d.). Epidemiologic studies demonstrated that the incidence of PCa is 1.56 times higher in the Black compared to the Caucasian population, and there is a lower PCa incidence in Asian countries, compared to USA and Europe, due to different diet and lifestyle, thus suggesting that PCa is triggered by environmental factors (Knudsen and Vasioukhin, 2010). Stress and obesity are additional risk factors and increase both incidence and grade of PCa (Bandini et al., 2017; Lv et al., 2019). Genetic predisposition is a significant risk factor in PCa development, and genetic alterations of hereditary prostate cancer (HPCa)-related genes, such as HPC1/RNASEL, HPC2/ELAC2, AR, as well as susceptibility genes, such as BRCA1, BRCA2, and several DNA mismatch repair genes, are responsible for the increase of PCa incidence by several folds (Gallagher et al., 2010; Noda et al., 2006; Urisman et al., 2012; Xu et al., 1998). Moreover,

there is a significant association between PCa risk and single-nucleotide polymorphism (SNPs) in genes that encode enzymes involved in the androgen pathways, like 5a-reductase-1 and 2, CYP17, CYP3A4, CYP19A1, as well as well as in genes involved in estrogen receptor signaling (Hernández et al., 2006; Margiotti et al., 2002; Sarma et al., 2008; Suzuki et al., 2005).

The mechanisms beneath the oncogenic transformation responsible for PCa initiation has been widely studied and several possibilities have been considered, from dedifferentiation and acquisition of immortality of terminally differentiated luminal cells to transformation of basal stem cells that begin to proliferate in an uncontrollable manner and constitute the bulk of the tumor featuring a luminal phenotype (Lawson et al., n.d.). The number of luminal epithelial cells increases in benign prostatic hyperplasia (BPH) but the appearance of columnar cells and cytology remain normal (Kristal et al., 2010). While hyperplastic condition is not considered a precursor of PCa, prostatic intraepithelial neoplasia (PIN), the *in situ* carcinoma, is considered a premalignant condition characterized by the dysplasia of PCa cells located in peripheral regions, accumulation of luminal cells, nuclear enlargement and decrease of basal cell layer integrity (Ayala and Ro, 2007). PIN is divided in high-grade and low-grade lesions. The transition from high-grade PIN lesions to prostate adenocarcinoma is triggered by several morphological changes: loss of basal layer, branching morphogenesis, enlargement of nuclei and nucleoli characterizing a cytologic atypia. Eventually, invasive epithelial cells proliferate in the peripheral zone of prostate gland inducing multifocal lesions (Knudsen and Vasioukhin, 2010). Androgen receptors (AR) are fundamental in the expansion of the luminal cell monolayer in PIN and cancer, and chemical castration by ablation of androgens usually de-bulks tumors (Huggins et al., 1941). Therefore, even if androgen-deprivation therapy (ADT) is initially effective in the majority of men

with metastatic PCa, metastatic disease tends to progress to CRPC with a variable timeframe (Seruga et al., 2011) (Figure 1).

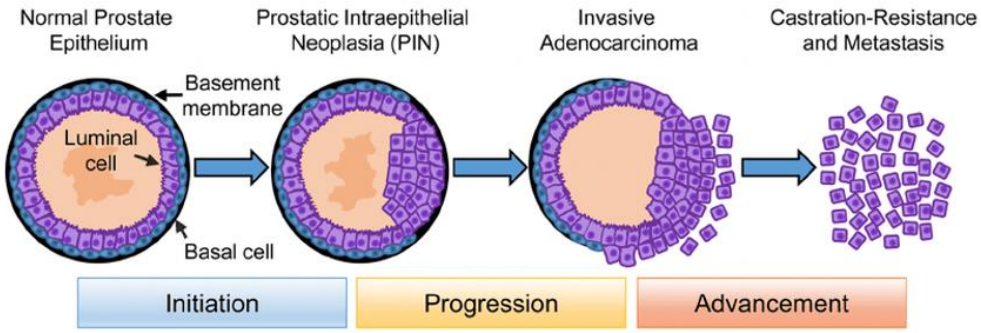

Figure 1. Schematic representation of prostate cancer initiation progression and advancement (Rybak et al., 2015).

Pathologist Donald F. Gleason developed PCa grading scheme known as the "Gleason Score" system, that has been refined recently to better define score grading. The grading is based entirely on the tumor growth pattern and architecture. Low grade tumors - Gleason Grade 1-3 - maintain organized ductal structures surrounded by stroma; high-grade tumors - Gleason Grades 4-5 - are characterized by disordered glandular architecture (Gleason and Mellinger, 2017). First Gleason grade is assigned to the most predominant pattern in the biopsy, the second Gleason grade is assigned to the second predominant pattern. The combination of Gleason pattern grading generates 6-10 score that indicate histologic variants and high-grade carcinoma (Humphrey, n.d.). The TNM staging system, that classify primary tumor (T), regional lymph node (N), and metastases (M), stratify patients according to the areas involved by the tumor. T stage describes 4 main stages of cancer – from T1 to T4 - and is divided into various subcategories indicating the different localization

of the lesions inside the prostate gland: *a)* T1 stage indicates that cancer is too small to be seen on a scan or detected during examination of the prostate; it is divided into a, b and c subcategories; *b)* T2 stage indicates that the cancer is inside the prostate gland and it is divided into a, b and c subcategories; *c)* T3 stage indicates that the cancer has broken through the capsule of the prostate gland and it is divided into a and b subcategories; *d)* T4 stage indicates that the cancer is spreading into other organs nearby. (N) describes whether the cancer has spread to the lymph nodes, and it includes subcategories N0 and N1. M describes the presence of metastasis in different parts of the body (M0-M1) defining the distance from the original tumor site through subcategories from a to c (Horwich et al., 2013).

Molecular events involved in PCa initiation and progression have been widely explored, and it is now clear that inflammation in the tumor microenvironment represents a crucial step: infiltrating immune cells like macrophages and lymphocytes induce the activation of IkappaB kinases (IKK)-alpha in prostate cells, that, in turn, stimulates proliferation and spread by repressing MASPIN, a noninhibitor member of the serine protease inhibitor superfamily (SERPIN) that repress cell motility, invasion and metastasis (Ammirante et al., 2010; Dzinic et al., 2017; Sager et al., 1996). Different epigenetic events are responsible for PCa initiation. Hypermethylation of several genes like RASSF1A, RABB2, MDR1, APC, and GSTP1 seems to be implicated in PCa development and characterizes prostate adenocarcinoma (Enokida et al., 2005; Nelson et al., 2009). Furthermore, molecular events - triggered by genetic alterations - promote neoplastic transformation: *a)* up to 70% of PIN lesions and 90–95% of PCa showed the decrease of GSTP1 expression, which seems to predispose luminal cells to increased oxidative damage, leading to accumulation of genetic changes (Lee et al., 1994); *b)* reduced expression of NKX3.1, that is highly expressed in luminal cells

and regulates the differentiation in normal prostate tissue, was found in 85% of PCa showing the loss of heterozygosity at chromosome 8p21-22, and in early stage disease, where it is linked to PIN development (Abdulkadir et al., 2002; Bethel et al., 2006). Chromosomal rearrangement and overexpression of ETS family proteins, such as ERG and TMPRSS2, are recurrent events in PCa that can be detected in up to 60% of PCa (Kumar-Sinha et al., 2008) and result in increased proliferation and tumor progression (Wang et al., 2008). Alterations in lipid metabolism pathway, in particular the overexpression of a-methylacyl-coAracemase (AMACR) and fatty acid synthase (FASN), are key events that promote PIN formation and invasiveness (Luo et al., 2002; Migita et al., 2009).

Tumors with Gleason grade ≥ 7 – likely characterized by high grade lesions, metastasis, and that frequently progress to a lethal form of PCa – present a panel of typical alterations that could lead to cancer recurrence. Indeed, the loss of PTEN is significantly correlated with Gleason and 1/3 of all castration-resistant metastatic PCa shows this deletion (Reid et al., 2010; Shen and Abate-Shen, 2007). FOXP3 results somatically deleted in PCa (Wang et al., 2009) while overexpression of SPINK1, that takes place in ETS fusion-negative tumors, is related with cancer aggressiveness and reduced progression-free survival (Tomlins et al., 2008). C-MYC, a transcription factor involved in cell-cycle and protein biosynthesis, results amplified in almost 40% of primary and 90% of metastatic PCa and correlates with clinical poor outcome (Ishkanian et al., 2009; Sato et al., 2006). The enzymatic component of polycomb repressive complex 2, EZH2, is prominently overexpressed in advanced PCa and its overexpression in localized PCa portends towards a poor prognosis (Varambally et al., 2002).

The castration-resistance of PCa, that is observed following surgical or chemical treatments downregulating AR signaling, represents the ability of cancer cells to maintain transcriptionally active AR despite the reduction of circulating androgens (Chen et al., 2009). Several mechanisms are responsible for castration-resistance of PCa: *a)* genetic mutations that increase the affinity of AR to progesterone and glucocorticoid hormones or that affect AR corepressors and activators, thus providing growth advantages to PCa resistant cells (Georget et al., 2002); *b)* splice variants of AR that provide a mechanism for escaping androgen suppression (Dehm et al., 2008); *c)* overactivation of kinases involved in AR phosphorylation, like MAPKs, Etk, and Pim1, that contributes to the transcriptional activity of these receptors (Giri et al., 2001; Kim et al., 2010).

PSA SCREENING: STRENGHTS AND LIMITATIONS

According to The National Cancer Institute (NCI), the 'biomarker' is as a biological molecule found in body fluids, blood or tissues that can be measured objectively and gives indications about the presence of a pathogenic condition. It can be used for screening, diagnosis or prognosis, for the evaluation of predisposition in developing a disease and for monitoring the response to therapeutic treatments (Ilyin et al., 2004). The major goal in this field is the identification of biomarkers that are able to detect the early formation of a tumor or metastasis and follow-through therapy efficacy (Gorges and Pantel, 2013).

The importance of the Prostate-Specific Antigen (PSA) in PCa screening is underscored by the fact that advanced or metastatic PCa was especially found in men who did not have regular PSA testing (Ohori et al., 1995). The kallikrein-related serine protease PSA is produced by the epithelial cells of prostate gland and,

although it is present in normal conditions, it results often elevated in PCa (Lilja, 2008). In blood, PSA exists in its free form (fPSA), representing the 5– 35 % of total PSA (tPSA), and in complex with serum protease inhibitors. fPSA exists in three forms: pro-PSA, benign PSA (bPSA) and intact PSA (iPSA) (Romero Otero et al., 2014). The percentage of free PSA, calculated as the ratio of fPSA over tPSA, was found to be lower in PCa patients, thus allowing a higher specificity in detecting cancer in men with high levels of PSA but normal DRE. However, since complexed PSA is more stable than fPSA, fPSA is not used as primary screening tool (Catalona et al., 1998). One-third of fPSA exists as pro-PSA, the inactive proenzyme form of PSA, which is normally cleaved by human kallikrein (hK), and it is more likely to be associated with PCa. A specific PSA isoform, characterized by a serine-arginine pro-leader peptide, has emerged as a prominent biomarker for PCa (Mikolajczyk et al., 2001; Romero Otero et al., 2014).The detection of abnormal PSA, that is an organ specific but not cancer specific biomarker, was set as less than 4 ng mL-1, with a diagnostic range between 4 and 10 ng mL-1 (Chen et al., 2004). Age-specific reference ranges were identified to improve test specificity since PSA production from benign epithelium increases with age, thus increasing the sensitivity of PSA for cancer detection in younger men, but reducing test sensitivity, even for early-stage and curable disease, in older men (Oesterling et al., 1995). Thus, some limitations of PSA as PCa biomarker are related to age-specific PSA production, increased PSA production by benign epithelium, as well as the challenge of identifying lymph node and bone metastases. Clinical studies showed that PCa progression is possible despite minimal serum PSA elevation, and a percentage of patients can develop metastasis in presence of undetectable PSA levels (Leibovici et al., 2007) (Figure 2).

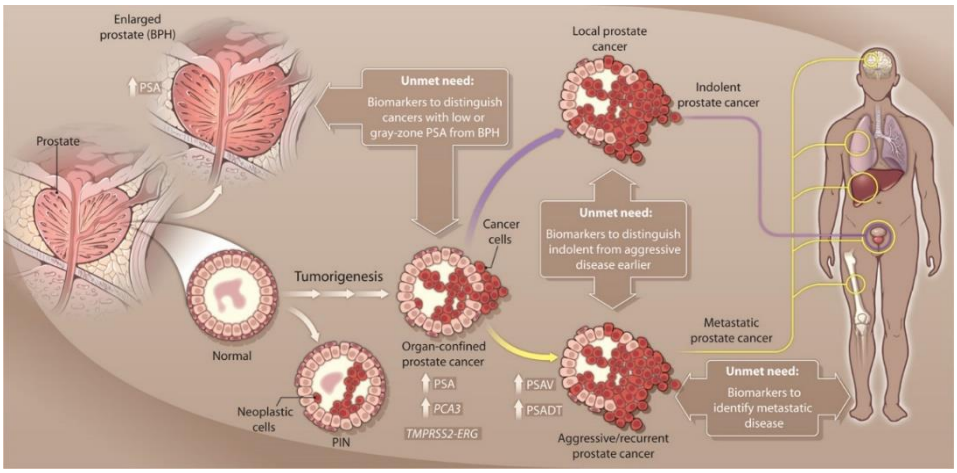

Figure 2. Challenges and unmet needs in prostate cancer biomarker research (Prensner et al., 2012).

NEW DIAGNOSTIC TOOLS IN PROSTATE CANCER DIAGNOSIS

In attempt to overcome the above-mentioned limits linked to PSA screening, new diagnostic tools have been developed to improve PCa early diagnosis. The prostate health index (PHI), calculated for each patient as phi= ([-2] proPSA/fPSA) × sqrt, is a test that is used in cases of men aged ≥50 years with a normal DRE and PSA levels in the range of 4–10 ng/ml. It is used to distinguish between cancerous and benign prostatic conditions and evaluate the need of biopsy, in order to improve PCa predictors accuracy (Houlgatte et al., 2012). Another interesting PCa biomarker, first reported by Bussemakers et al. in 1999, is the prostate cancer antigen 3 (PCA3 or DD3), that is a long non-coding RNA of unknown function encoded by a gene located on chromosome 9q21-22 (Bussemakers et al., 1999). DD3 is useful for PCa detection since it is not expressed in normal prostate tissue, while it is detected in >95 % of the primary and metastatic cases (Sartori and Chan, 2014). Progensa PCA3 test' (Hologic), an *in vitro* amplification test approved by

the US FDA in 2012, is carried out in post DRE urine specimens of PCa patients and calculate the PCA3 score based on the ratio between PCA3 and PSA RNA levels. Scores lower that 25 indicate a reduced possibility of PCa presence (Auprich et al., 2011). Non-FDA approved PCa biomarkers are available as Clinical Laboratory Improvement Amendments-based laboratory (CLIA) developed tests (Cary and Cooperberg, 2013). An example is TMPRSS2-ERG gene fusion test, which detect *TMPRSS2:ERG* rearrangement. Although some reports showed that people testing positive to this test had a more aggressive PCa, with higher metastatic potential and increased mortality risk (Schoenborn et al., 2013), some other studies did not confirm this correlation (Vlaeminck-Guillem et al., 2010). Due to this limitation, TMPRSS2-ERG gene fusion is usually combined with PCA3 evaluation (Leyten et al., 2014). The Oncotype DX PCa test is a multi-gene expression assay based on 12 cancer-related genes representing four different biological pathways involved in PCa: androgen pathway (AZGP1, KLK2, SRD5A2, RAM13C), proliferation (TPX2), cellular organization (FLNC, GSN, TPM2, GSTM2) and stromal response (BGN, COL1A1 and SFRP4). The test is developed for formalin-fixed paraffin-embedded (FFPE) diagnostic prostate needle biopsies containing as little as 1 mm of prostate tumor and seems to be a good predictor of aggressive PCa, as well as a valuable indicator for PCa risk stratification (Knezevic et al., 2013). Similar tests, based on different technologies (*i.e.* ConfirmMDx test, Prolaris test, 4K score test, etc.), have been developed to avoid unnecessary biopsies in low-risk patients and lead the clinicians to an easier management decisions (Saini, 2016).

The research of an ideal biomarker easily detectable in body fluids and not present in healthy people ran up against biomarkers intrinsic limitations. Indeed, the idea of a single useful biomarker has been replaced more and more by the search for a panel of analytes, since variation in a single biomarker is not sufficient to identify

disease presence or progression, that usually results from a large number of alterations (Califf, 2018). The opportunity to exploit novel potential biomarkers for PCa diagnosis has recently emerged. In particular, there is a growing interest in PCa-related free miRNAs to be used as diagnostic and prognostic tool, as they could overcame most of the challenges of currently used PCa biomarkers.

CIRCULATING MIRNAs AND PROSTATE CANCER

Blood-based biomarkers are diagnostic and prognostic tools widely used by clinicians for evaluation of different diseases, including cancer. Since disease establishment and progression involve a large number of processes, the identification of clinically-useful and specific biomarkers could be similar to "finding a needle hidden in a haystack" (Kumar et al., 2006). Among blood-based biomarkers, microRNAs (miRNA), which are stable and easily detectable in body fluids like blood and plasma, can potentially be used as noninvasive markers for cancer detection (Ganepola et al., 2014).

MiRNAs are ~22 nucleotide long noncoding sequences of RNA that are located across the genome, within an intron or untranslated region (UTR) of coding gene (Rodriguez et al., 2004). Pri-miRNAs are transcribed from their genes in longer primary transcripts that may be hundreds to thousands of nucleotides in length and are processed by two Rnase III proteins - Drosha and Dicer (Lee et al., 2003). Canonical and non-canonical miRNA biogenesis pathways lead to the splicing, capping and polyadenylation of pri-miRNA and the formation of a functional miRISC complex that binds to at the 3′ UTR of their target mRNAs to induce degradation and translational repression (Hayder et al., 2018). The targeting of

mRNA regions in the 5′ UTR and in coding sequence within promoter also seem to induce the silencing of gene expression (Xu et al., 2014) (Figure 3).

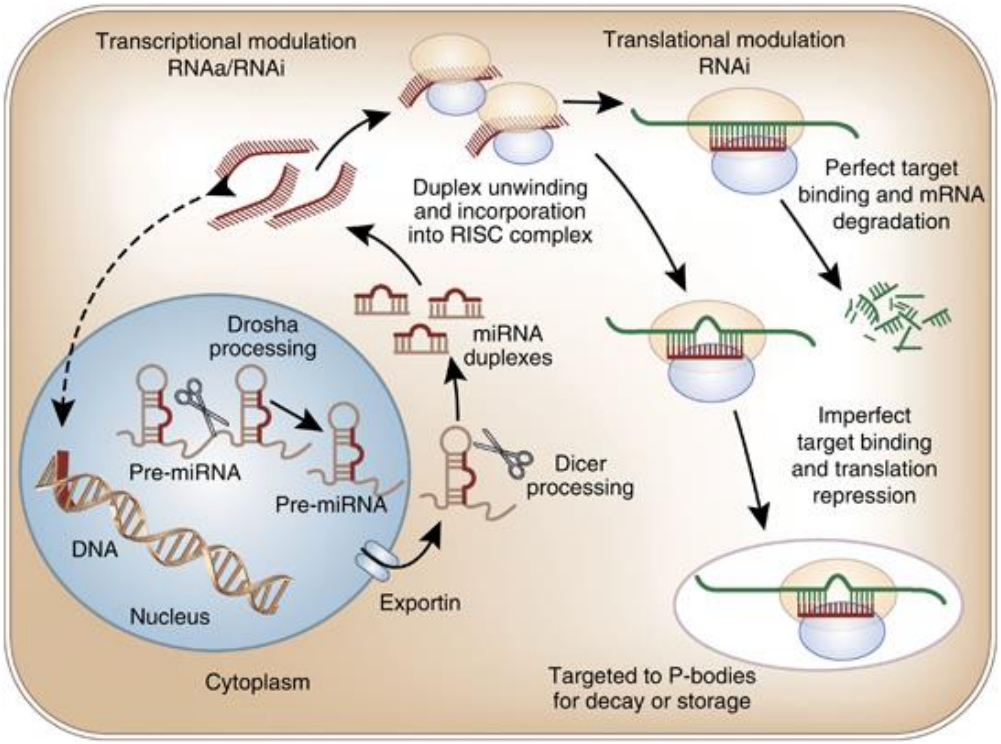

Figure 3. MicroRNAs biogenesis and mechanism of function (Chandrasekaran et al., 2012).

MiRNAs reflect cell status in terms of proliferation, cell cycle, differentiation and apoptosis since they play an important role in regulating fundamental genes involved in both physiological and pathological processes. MiRNA tissue specificity allow also the identification of the origin site from which they are released (Punnoose et al., 2010). Extracellular miRNAs seem to derive from multiple sources. They can result from lysis of death cells and apoptotic bodies or from living cells active release through lipoprotein complexes, microvesicles, lipid-membrane vesicles and exosomes, that assure a high stability from enzyme degradation (Kishikawa et al., 2015). Up to 500 copies of individual miRNAs have

been found per cells, while lower levels of miRNAs were detected in biological fluids and extracellular environment (Liang et al., 2007; Pritchard et al., 2012). In 2005, Yang et al. showed the vital importance of miRNA network through the homozygous deletion of the gene coding for Dicer - the key enzyme of miRNA biogenesis - that resulted in the disruption of prenatal development of murine embryos (Yang et al., 2004). Murine knock-out models for miRNA maturation enzymes and complexes elucidated the role of miRNAs in cell function and homeostasis and their crucial role in embryonic stem cell self-renewal and development (Bernstein et al., 2003; Park et al., 2010; Wang et al., 2007). The diagnostic and therapeutic potential of miRNAs was showed in later studies that pointed out the accessibility of miRNAs circulating in patients serum and the correlation of miRNA patterns with many types of diseases (Izzotti et al., 2016; Lawrie et al., 2008; Pasquinelli et al., 2000), including cancer, where tissue specific miRNAs are either downregulated (Calin and Croce, 2006; Chang et al., 2008) or overexpressed (Hayashita et al., 2005; Tagawa and Seto, 2005). Indeed, several lines of evidence have shown that miRNAs are crucial in modulating host immune response, tumor growth and progression, as well as metastasis spread (Ruivo et al., 2017). Many clinical trials, initiated on the heels of increasing publications, proved the applicability of miRNAs in cancer diagnosis and prognosis (Izzotti et al., 2016; Russo et al., 2018).

Several studies have investigated the potential application of circulating mRNAs and miRNAs in PCa. In particular, miR-200b-3p resulted downregulated in hyperplasia and in healthy adjacent tissues compared to PCa samples, and could be useful, in combination with miR-181b-5p, to differentiate BPH and PC (Pełka et al., 2021). The deregulation of specific patterns of miRNAs (*i.e.* miR-141-3p, miR-221, miR-21 and miR-375) appears to be correlated with PCa initiation and

progression (Bryant et al., 2012). A comprehensive analysis of serum miRNA expression profiles of 809 cases of PCa and 241 cases of negative prostate biopsy performed on a standardized microarray platform identified the upregulation of serum miR-17-3p and miR-1185-2-3p in patients with PCa, with a distinct profile from that observed in BPH specimens (Urabe et al., 2019). Another study conducted on 20 patients – with mean age of 68.6 years and a mean PSA of 21.3 ng/ml – and 8 healthy patients showed that the relative serum expression of miR-106b, miR-141-3p, miR-21 and miR-375 was significantly increased in PCa patients compared to healthy controls, thus indicating the potential possibility of discriminating PCa patients from healthy controls by detecting miRNAs (Porzycki et al., 2018). Notably, mir-375 serum levels resulted higher in patients with disseminated or CRPC compared to those measured in patients with a localized tumor, thus providing information about tumor clinical aggressiveness (Brase et al., 2011). Likewise, elevated levels of circulating miR-182-5p were associated with advanced PCa (Bidarra et al., 2019).

The stability of miRNAs in various body fluids along with the development of specific high-throughput detection methods allowing miRNA detection in extracellular fluids are among the main advantages of using miRNAs as circulating biomarkers. In fact, human fluids are specimens easily accessible without invasive procedures, thus suggesting that circulating miRNAs could represent a unique source material for clinical diagnostics (Turchinovich et al., 2011). To this end, microarrays and new qRT-PCR-based strategies have been developed to achieve a more rapid and sensitive detection of circulating miRNAs by reducing the number of amplification cycles and exploting different probes such as molecular beacons, enzymatic luminescence, nanoparticles-based probes and circular exponential amplification (Kelly et al., 2015). However, significant challenges remain, such as

the low concentration of miRNAs released in blood, especially in the early-stage disease, and the difficult localization of the biomarker release site (Hindson et al., 2013; Witwer, 2015). In recent years, ultrasound-based techniques have been proven useful tools in the field, that could help to overcome some of the biomarker-related limitations and advance their clinical application.

ULTRASOUND MECHANISMS

The mechanisms at the basis of ultrasound (US) techniques are sonoporation and the transient permeabilization of cell membrane resulting from the physique phenomenon named “cavitation”. Cavitation is induced by the formation of a variable number of pores on the membrane caused by the growing and shrinking as well as the total collapse of gas-filled microbubbles present in cell medium. The use of commercial available microbubbles, approved as contrast agents, could enhance this phenomenon by amplifying the biophysical effects of US (Lentacker et al., 2014). The exposure to US waves changes the physiologic state of cell membrane inducing deformation, local temperature increase and other chemical and mechanical effects, which result in the increase of cell permeability and the establishment of an enhanced bidirectional efflux, thus facilitating both the uptake and the release of low weight molecules like drugs, peptides, proteins and nucleic acids, through cell membrane (Frenkel, 2008).

Therefore, there is a wide range of biological effects produced by US exposure, which are dependent on the intensities of US waves applied to biological systems. In fact, during the cavitation, microbubbles are subjected to a gas influx and efflux that cause an alternate phase of expansion and compression. At low acoustic pressures, a stable cavitation produces the symmetrical oscillation of microbubbles,

with an equilibrium of the net gas influx (Figure 4). These fluctuations result in the generation of a microstream in the nearby liquid and in a series of pushing and pulling forces against cell membrane producing mechanical stress which could allow the entering of the bubble through the bilayer. At higher intensities, the expansion phase extends since the microbubble reach its resonant size or, according to the US parameters applied, collapses asymmetrically generating shock waves or jets of liquid that, in proximity of the cell, produce shear stress that disturbs membrane integrity (Sboros, 2008; VanBavel, 2007). This phenomenon is called inertial cavitation and it has been shown that it could enhance intracellular delivery of drugs and molecules (Miller et al., 1999) (Figure 4).

Both mechanisms are responsible for changes in cell bilayer and, in the case of inertial cavitation, of membrane disruption. Pore formation is one of the most frequent event that occurs during US treatment, even if several studies reported the activation of endocytosis processes after pulsed US exposure (Lionetti et al., 2009).

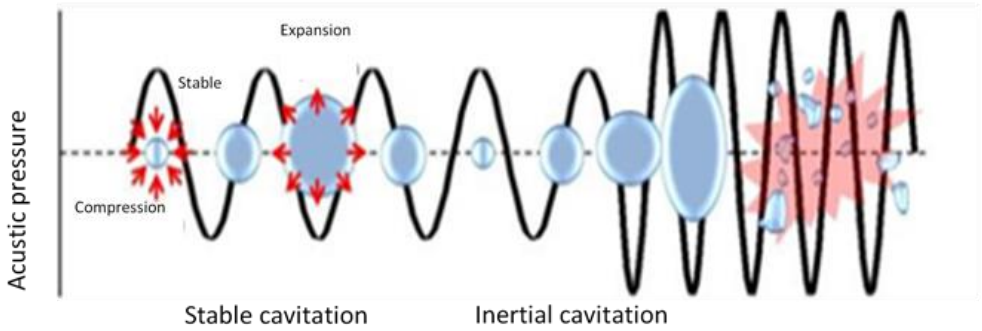

Figure 4. Ultrasound wave behavior during stable and inertial cavitation (Liu et al., 2014).

BIOLOGICAL EFFECTS OF ULTRASOUND

The application of focused US can locally modify tissue integrity with low off-target effects. The generation of US-induced bubbles mechanically disrupt tissues, inducing a wide range of effects ranging from cavitation-based permeabilization to complete tissue liquefaction. Tissue damage can be managed controlling US application parameters on the basis of the approach used and the final effect wanted (Lucchetti et al., 2020).

The induction of mechanical and chemical events responsible for pore formation and cell permeabilization has been well understood through studies aimed to study single cell behavior under US waves effect (Figure 5). To this end, defolliculated Xenopus laevis oocytes were subjected to an ultrasonic field to analyze formation, size and time of resealing of pores on cell membrane through the inward transmembrane current (TMC). TMC technique measures the change of the ion transport through the non-specific pores, resulted from ion concentration and electrical potential gradient across the membrane, thus quantifying the contribution of Na^+, K^+ and Cl^-. The comparison between TMC and control values allowed the identification of the size of the generated pore, that ranged from 50-2500 nm, and indicated the effective time necessary to induce pore formation and resealing (Zhou et al., 2009). A detailed analysis of the highly complex dynamic of single cell sonoporation and US-mediated drug delivery was performed through US treatment of HEK 293 cells combined with microbubbles contrast agents (1-3 um) and monitored with whole cell patch-clamp and ultrafast fluorescence microscopy (Fan et al., 2012). Streptavidin-coated microbubbles allowed to better understand the interaction of a single microbubble with specific cell receptors on cell surface. Transient cell membrane modifications during the sonoporation were monitored

with TMC and Propidium Iodide (PI) fluorescence, and cell viability assay on calcein-AM was used to verify the recovery of cell membrane integrity after the treatment. TMC studies of pore formation and size highlighted two different mechanism of pore resealing that occur after sonication: a faster one that involve membrane fusion and exocytosis events for repairing small membrane disruption, and a slower one associated with more extensive mechanical injury repair. Variations of these recovery constants were linked to structural differences and membrane heterogeneity among different cell types. The study pointed out that cell response to US treatment depends on both acoustic pressures applied and bubbles radius. In fact, tuning the US application showed that smaller bubbles excitation generates less PI uptake than larger ones, since pores radius is strictly related to microbubbles size with a direct proportion. Based on fluorescence imaging and calcium influx measurements, it was clear that there is an inversely proportion between acoustic pressures and microbubbles size resonance. In fact, increasing pressures excited even smaller bubbles. A model of Multidrug Resistance Protein-1 (MRP1) was used for the analysis of delivery and efflux of membrane-impermeable compounds, that need uptake and efflux pumps. The model compared the behavior of HEK-MRP1 positive cells and parental cells not expressing MRP1 under US treatment. The efflux rate of fluorescent MRP1 was eight times faster for HEK-MRP1 compared to parental cells during sonication, confirming that US enhance transporter-induced efflux (Fan et al., 2012).

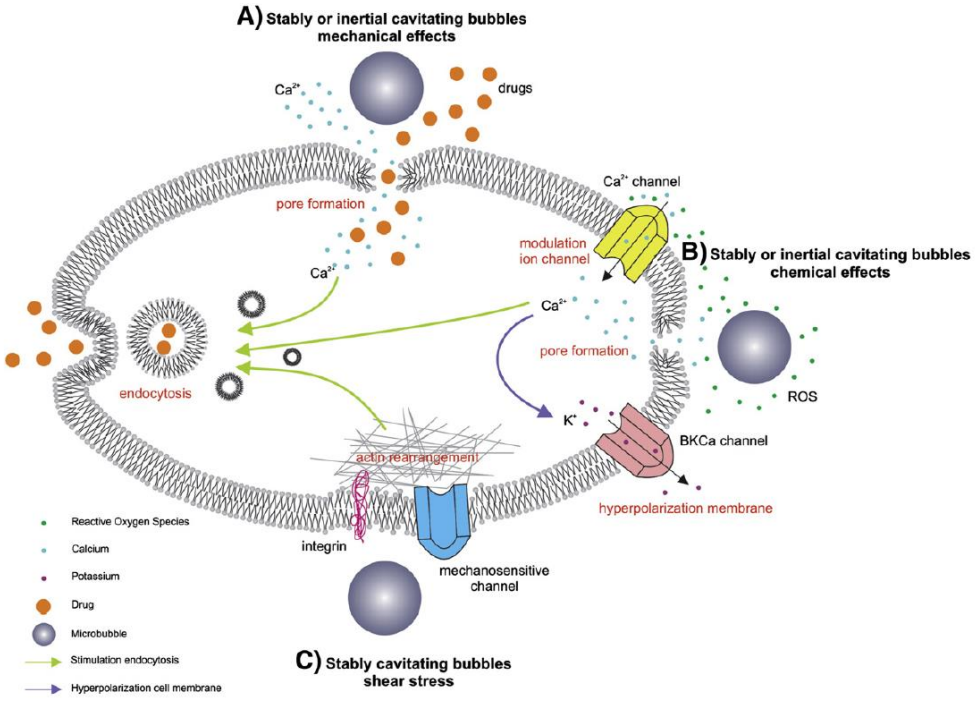

Figure 5. Ultrasound application and effects on cell physiology (Lentacker et al., 2014)

ULTRASOUND TREATMENT FOR BIOMARKERS RELEASE

Single-cell studies furthered the understanding of the mechanism of pore formation and resealing, the involvement of active transport and molecules uptake and release through membrane bilayer during US treatment. Based on all the available evidence, it became clear that US treatment was applicable on more complex system both *in vitro* and *in vivo*. In 2009 D' Souza et al. demonstrated that the application of an appropriate amount of ultrasonic energy to tumor site promotes the release of specific markers from tumor cells. *In vitro* study on colon cancer cells LS174T showed a progressive increase of CEA release after US exposure with a low death rate at power levels below 1W/cm^2. The direct application of US to the site of tumor in mice bearing LS174T xenografts caused a significant change in blood CEA levels compared to those measured in control groups, which were composed of no tumor-bearing mice and tumor-bearing mice treated in a no tumor

site (D'Souza et al., 2009). Later, in 2018, D' Souza et al. further demonstrated the applicability of this technique to tumor of unknown origin through the detection of multiple nucleic acids and proteins released in the bloodstream. In addition to increased CEA release, LS174T- US treatment at varying intensities caused a significant increase of CA19-9, mir-16 and mir-141, in terms of number of copies present before and after the treatment. PCa cells LNCaP were also exposed at the same US treatment, as done for LS174T. PSA and mir-16, mir-141, mir-200c quantification showed a progressive increase that reached significance at 0,7 and 1 W/cm^2 treatment (D'Souza et al., 2018). US treatment was also applied to a colon cancer orthotopic model in the liver. Tumor was sonicated by direct application of transducer on the area of the tumor. A significant difference in CEA and CA-19-9 release and in microRNAs levels was observed between pre and post treatment samples when compared with control groups. Similar sonication conditions were applied to the liver, showing an increase in protein levels after the sonication compared to control groups. D' Souza et al. extended the investigation to patients exposed to MRg-FUS of uterine fibroids by analyzing specific markers in blood samples collected before and after the treatment. Endothelin 1 and CA125 raised significantly after MRg-FUS, and their levels correlated with the volume of the ablated fibroid. Only 5 patients out of the 16 showed an increase in miRNAs levels, in particular mir-21, mir-363 and mir-490 (D'Souza et al., 2018). Chevillet et al. applied three pulsed focused US treatments on rodent PCa xenografts in order to produce mild heating, permeabilization or liquefaction of the tissue and evaluate the release dynamics of tumor-derived miRNAs for each condition. The analysis of miRNA profiling on blood specimens highlighted how much important is the time factor in this kind of experiments. In fact, the maximum plasma abundance for most miRNAs of interest was observed at 15 min, with a gradual decrease over 30

minutes, and returning to the baseline at later timepoint. The same kinetic trend was observed in liquefaction and permeabilization regimens. Another remarkable consideration was that the intensity of the treatment is directly proportional to the magnitude of the effects and amount of biomarker released. Indeed, the liquefaction treatment, that provoked the real boiling of the tissue and induced a high and rapid rate of biomarkers release, is applicable only for a restricted range of clinical situations, where the integrity of the tissue is not required. Instead, the cavitation-based permeabilization regimen produced a confined tissue damage, quite similar to the one produced by a normal biopsy. This suggest that this technique could be suitable for the interrogation of at-risk tissue in individuals with cancer genetic predisposition (Chevillet et al., 2017).

Off-target effects of low-intensity ultrasound (LIPUS), ranging from 650 to 4500 kHz, were explored in colorectal cells (Lucchetti et al., 2020). LIPUS treatment affected cell proliferation, that resulted drastically reduced after high intensity treatment (60%), while an increment of ALP activity, a marker of colorectal cells differentiation, was measured in CaCo-2 cells at 650 and 1000 kHz. LIPUS seemed to reduce epithelial-to-mesenchymal transition (EMT), inducing an increase of E-Cadherin and a decrease of Vimentin expression. Moreover, wound healing time shortened both in HT29 and CaCo-2 cells, with a direct correlation with the frequency used. Higher frequencies (1000 kHz, 2400 kHz and 4500 kHz) induced a reorganization of cell cytoskeleton through the alteration of actin fiber coherency and the formation of filopodia-like protrusions. Moreover, LIPUS treatment increased the extracellular vesicles (EVs) biogenesis release and uptake, as confirmed by a cytometry-flow based method, showing its potential applicability in liquid biopsy, as EVs are well-known carrier of molecules of interest, such as DNA, RNA and microRNAs (Lucchetti et al., 2020).

The US-mediated membrane permeabilization is enhanced when microbubbles or nanobubbles are added in cell culture medium and the size of the bubbles used is very important since it is strictly linked with the ability of extravasation through tissue and cells. Paprosky et al. compared the use of microbubbles and perfluorocarbon phase-change nanodroplets in promoting the release of mammaglobin mRNA and mir-21 from breast cancer cells, both *in vitro* and in a murine xenograft model, by using three different instruments with growing intensities combined with either microbubbles, droplets or simple medium. Fluorescent labelled contrast agents allowed the localization of nanodroplets and microbubbles in relation to the cells by confocal microscopy. The use of hydrogen peroxide treatment as a control enabled the authors to see the amount of released biomarkers resulting from cell death. The choice of mammaglobin, that was not expressed in the model, permitted to demonstrate *in vivo* that the increase of the protein was uniquely due to the insonation of breast cancer grafts. In the study emerged that nanodroplets are less stable than microbubbles, especially in *in vivo* models, due to the possibility that a population of droplets, due to their proximity, resulted in a large bubble cavitation nucleus, inducing effects in biomarkers release and cell death quite similar to the ones achieved with microbubbles. Diversity in miRNA and mRNA release was ascribed to differences in their endogenous levels; in this case, the number of copies, as well as the size of the nucleic acid, were related to their ability of exit cell membrane. Once again US duration, that is strongly related with US energy amount, was a key factor in determining markers release and cell death (Paproski et al., 2014). The exposition of tumors to high intensity focused US in presence of nanodroplets could amplify the release of EVs carrying relevant tumor-specific biomarkers into adjacent blood vessels. HT1080-GFP tumors in chicken embryos exposed to a combination of nanodroplets and US

demonstrated for the first time that nanodroplets and focused US stimulate the release of large numbers of EVs from tumor cells into the bloodstream, allowing enhanced detection of relevant protein, mRNA, miRNA, and DNA biomarkers containing tumor-specific mutations which are of great diagnostic value (Paproski et al., 2017).

However, US-mediated membrane permeabilization is a process that needs to be finely monitored, since the resealing and maintenance of membrane integrity is necessary to cell viability and proliferation. The analysis of membrane protein patterns before and after sonication in US-induced hemolysis experiments illustrated that the sonication could induce severe and irreversible membrane disruption, leading to degradation of membrane proteins, maybe weakening the bilayer, and inducing a more important membrane damage. The presence of plasma seems to protect membrane proteins, but the mechanism has not been clarified yet. This consideration underlines that cellular and molecular US-induced damages could be the result of different mechanisms (Kawai and Iino, 2003). Furthermore, a study on leukemia cells described some factors that could lead to US-induced apoptosis: *a)* the sonication intensity; *b)* the ultrasound-induced DNA fragmentation; *c)* the decrease in mitochondrial transmembrane potential and increase in intracellular superoxide production. Thus, since some US treatments aim for cell death but others require the maintenance of cell viability and proliferation, it is fundamental to optimize US parameters in order to achieve treatment goals (Ando et al., 2006). The risk of tumor dissemination after US treatment is another aspect that needs to be taken in consideration since the sonication could induce the release of viable malignant cells and may alter cytokines pattern, thus either allowing or suppressing the formation of metastasis (Xing et al., 2008). Although further investigations are needed to clarify the

aforementioned points, the growing bulk of evidence in literature showed that the application of US treatment on cells and tissues could be exploited to enhance molecules release, thus allowing the identification of specific biomarker signature for disease diagnosis and prognosis.

ULTRASOUND TREATMENT FOR DRUG DELIVERY

The application of ultrasound can exert a wide range of thermal and non-thermal effects, such as cavitation and acoustic streaming. These biophysical effects produce the permeabilization of cell membrane that enhance not only the release, but also the delivery of molecules. A number of factors in the tumor microenvironment, as well as the features of macromolecules and nanoparticles used, like molecular weight or physical size and electrostatic charges on the surface, can reduce the levels of delivered anti-cancer agents (Wang and Yuan, 2006). By enhancing the entry of molecules of interest, such as DNA, proteins and drugs, in specific cells and tissues, US could overcome several limitations often linked to cancer therapy and enable a non-invasive and precise delivery of drugs to the lesion, thus allowing the optimization of the administered dose (Lentacker et al., 2014).

The enhanced transfer of DNA via US treatment was assessed both *in vitro* and *in vivo* using a system of e β-galactosidase and luciferase DNA reporter plasmids. The transfection rate of cancer cell lines constantly increased up to a 220-fold with the increase of pressure amplitude and reached the plateau after 3 minutes of sonication. Focused US treatment applied after intratumoral DNA injection, induced a 10-fold increase in the number of β-galactosidase positive cells analyzed by histology and a 15-fold increase of β-galactosidase protein expression measured by ELISA assay (Huber and Pfisterer, 2000). Well established methods applied in gene editing and

expression modulation can be greatly enhanced using microbubble preparations, that can serve as nucleic acids vehicles, since it was demonstrated that oligonucleotides were bound to microbubbles shell (Porter et al., 1996; Unger et al., 2001). The membrane permeability triggered by US can facilitate the delivery of plasmid-encoded transgenes with a wide range of effects on tumor site: the replacement of a suppressor genes exploiting nanoparticle mediated delivery (Gaspar et al., 2011), down regulation of oncogenes with small interfering RNA (Zhang et al., 2006), genes encoding enzymes capable of drug activation (Won et al., 2011), introduction of genes encoding immunological mediators (Zhu et al., 2010) and introduction of genes that prevent angiogenesis (Belur et al., 2011).

Karshafian et al. investigated how the size of delivered molecules (ranging from 10kDa and 2MdDa), US parameters and microbubbles shell affect reversible permeability induced by US treatment and if sonication affects long term cell viability and proliferation. The use of FITC-dextran and PI assay revealed that 80% of cell population is reversible permeabilizated after US treatment with a proportional increase of permeability with the growing of both acoustic pressures and microbubble concentrations, reaching a maximum beyond which the permeability decreases. PI staining after sonoporation highlighted that reversible permeabilization does not affect cell viability and proliferation. Long-term viability assessed by clonogenic cell survival assay, indicated that 30-50% of cells maintain proliferative ability. Pore size of 56 nm allowed the delivery of 2MDa molecules, and the presence of microbubbles significantly increased the efficiency of delivery. The type of microbubbles influenced the concentration at which the maximum permeability was achieved: lipid and proteic shell microbubbles have been compared, and lipid smaller microbubbles needed higher concentrations to induce an effect of permeabilization compared to the larger protein ones. The size of

microbubble is a fundamental parameter as it is strictly linked to bubble resonance frequency and consequent oscillation and disruption that lead to the formation of microstream, shear stress and pores formation on cell membrane (Karshafian et al., 2010).

Delivery of liposomes containing doxorubicin (Dox) and fluorescein-isothiocyanate (FITC)-dextran (molecular weight 4 to 2000 kDa) was investigated on HeLa cells at different acoustic power generated by a transducer at 300 kHz by using flow cytometry and confocal microscopy. The study revealed that US treatment induced the uptake of doxorubicin and dextran via a combination of endocytosis and permeabilization mechanisms. The delivery as well as the percentage of cells internalizing molecules increased with the increasing of the ultrasound beam power, or mechanical index (Afadzi et al., 2013).

These studies have demonstrated how US treatment applied on biologic systems could be a useful tool to manipulate single cells and tissue environment as well as their content. The possibility of controlling the impact of US on the physiologic cell condition without causing drastic morphologic changes suggests that US could provide a promising, non-invasive method for biomarkers detection and drug delivery.

MATERIAL AND METHODS

CELL CULTURE

LNCaP, DU145, PC3 and 22Rv1 PCa cell lines were purchased from American Type Culture Collection (ATCC). Cells were cultured in a humidified incubator in 5% CO2 at 37°C. DU145 and PC3 were cultured in RPMI-1640 medium (#30-2001, ATCC) supplemented with 10% Fetal Bovine Serum (FBS), (certified, One Shot™ format, United States); 22Rv1 were cultured in Dulbecco's modified Eagle's Medium (DMEM) with 10% FBS; LNCaP were cultured in RPMI 1640 with 10% FBS supplemented with 10 mM HEPES (#ECM0180D, Euroclone) and 1mM Sodium Pyruvate (#ECM0542D, Euroclone). All media were supplemented with antibiotics (150 U/mL penicillin, 200 U/mL streptomycin) (#ECB3001D, Euroclone) and 2 mM Glutamine (#ECB3000D, Euroclone). All cell lines were routinely tested using PCR Mycoplasma Detection Set (#6601, Takara). Cell line authentication (STR) was carried out.

ULTRASOUND INSTRUMENT AND SONICATION PROTOCOLS

The sonication was performed with Sonowell® (Promedica Bioelectronics S.r.l.) (Lucchetti et al., 2020), designed to operate on standard plate-wells. Our version has 4 flat transducers of 12mm diameter, frequencies 0.65, 1.0, 2.4 and 4.5 MHz, whose emissions are controlled with a 4-channel generator/amplifier operating in parallel. The instrument is equipped with a thermostatic tank controlling the sample temperature is kept constant at 37°C. A robotic x,y,z system provides the controlled plate-well displacement on the transducers. The set-up is of the type well-on-

transducer (Hensel et al., 2011) with the plate inner side bottom end calibrated to be 1 mm below the Near/Far Field plane (N/F Field). The geometry of the transducers positions the N/F Field plane at the same Z quote for all the frequencies, ensuring that all the samples experience the sonication wavelets at the maximum of the excitation profile, so that the sample solution is homogeneously sonicated in the Far Field. Protocols of sonication have been set with the instrument software SonoWell Soft©, which allows the simultaneous use of 4, 2 or 1 transducer on the same well plate. Our experiments were optimized on Falcon 24-well plates. Calibrations of the acoustic pressure used in the experiments were performed using a needle hydrophone (0.5 mm) preamplifier and DC coupler (Precision Acoustics, UK), monitoring the amplitude of the negative peak detected signal with a Fluke Scopemeter 125. Calibration curves of mW/cm2 vs acoustic pressure kPa measured, were obtained for all the transducers over the range of 0.010-6.0 W/cm^2.

HOMOGENEITY OF WELL SURFACE COVERAGE

Evaluation of homogeneity of transducer wavelet transmission over the cellular layer adhered was established using DU145 cells plated at confluency in a 24-well plate and treated with US at 500 kPa acoustic pressure, 650 KHz, 1 MHz, 2,4 MHz and 4,2 MHz. Cells were stained with Crystal Violet (0,2%, #C0775, Sigma-Aldrich) and ImageJ software (Schneider et al., 2012) was used to evaluate the percentage of well surface coverage. Homogeneity of detachment profiles were evaluated comparing images before and after sonication.

ULTRASOUND TREATMENT

PCa cells were plated in 24-well plate (Falcon) at concentration of 150.000 cells/well. Cell layers were rinsed with PBS after either 24 (22Rv1, DU145, PC3) or 48 (LNCaP) hours of incubation with complete media; then, fresh media was completed with exosomes-depleted FBS to eliminate interference of RNA-containing exosomes from FBS, and protease inhibitors were added to avoid PSA degradation by intracellular proteases released following US treatment (#04693159001, Roche). Supernatant samples were collected before and after the sonication from the same well; incubation time for untreated (D'Souza et al., 2018) control cells was equal to sonication period. Top sealing films were applied to plates, covered with ultrasound coupling gel and a layer of phono absorbent material. The frequency of 1MHz was selected for the treatment of all cell lines as previously reported (D'Souza et al., 2018). DU145, PC3 and 22Rv1 were treated at 1MHz of frequency (Ispta 410.5 mW/cm^2), 10% DC for 15 minutes, 30 minutes and 1 hour; LNCaP were treated with the same parameters at lower intensities (Ispta 307.9 mW/cm^2) to avoid detachment of cell monolayer. Duty cycle was maintained below 20%, since higher percentages caused membrane disruption and morphological alterations. Samples were centrifuged for 30 min at 1500 x g to remove detached cells and debris and processed for protein and miRNA quantification.

Drug delivery experiments were performed on DU145 cells plated the day before at the concentration of 30.000 cells/well by adding a scramble (SCRB) D-tripeptide (Tornatore et al., 2014) conjugated with fluorescein isothiocyanate (FITC) at the final concentration of 25 uM in 250ul of Opti-MEM® Reduced Serum Medium (# 31985062, Gibco) with two different ultrasound regimens: a short-time higher pressure-treatment (1MHz, DC 10%, Ispta 410.5 mW/cm^2 , 500

kPa, for 3 sec, 30sec, 60 sec) and a long-time lower-pressure treatment (1MHz, DC 10%, Ispta 307.9 mW/cm^2, 250 kPa, for 180 sec, 300s, 600 sec).

PROTEIN QUANTIFICATION

Culture media of PCa cells were analyzed for PSA concentration using ELISA kit Human Prostate Specific Antigen (PSA) ELISA kit (#EA100981, Origene). PSA standards (1,56 ng/ml, 3,12 ng/ml, 6,25 ng/ml, 12,5 ng/ml, 25 ng/ml) were provided from the kit.

RNA EXTRACTION AND RT-qPCR

RNA extraction and quantitative real-time polymerase-chain reaction (RT-qPCR) Total RNA was isolated using TRIzol Reagent (RiboEX™, Cat. No. 301-001, GeneALL®, Seoul, Korea). The isolated RNA was spectrophotometrically quantified, and equal amounts were used for cDNA synthesis using HighCapacity cDNA Reverse Transcription Kit (#4368814, Applied Biosystems™). RT-qPCR performed by using Luna® Universal qPCR Mastermix (#M3003X, New England Biolabs). Primers for prostate specific antigen (PSA) spanning exon 1-2 were purchase from IDT (S:5'-AACCAGAGGAGTTCTTGACCCC-3', AS:5'-GAACTTGCGCACACACGTC-3').

MiRNAS EXTRACTION

MiRNAs extraction from supernatants, collected before and after sonication, were carried out with Plasma/Serum RNA Purification Mini Kit (#55000, NORGEN

BIOTEK. CORP) according to manufacturer's instructions. Briefly, supernatant samples were collected and centrifuged for 10 min at 1500 x g at 4°C to remove detached cells and debris. 5 ml di C. Elegans spike-in control miRNAs concentrated 5 fmol/ml, were added before extraction of total miRNAs. miRNA concentrations and qualities were evaluated by using NanoDrop 2000 (Thermo scientific, USA). MiRNAs quantification in cell supernatants was measured by using TaqMan RT-qPCR. The results were standardized to the spike-in control C.elegans miRNAs (#000200). Taqman single tube assay for miR-16-5p (#000391), miR-200c-3p, (#002300) and miR-141-3p (#000463), miR-629-5p (#002436), miR-374a-5p (#000563), miR-194-5p (#000493) and let-7d-5p (#002283) were purchased from Thermo-Fisher. miRNA expression profiling was performed using TaqMan™ Advanced miRNA Human Serum/Plasma RT-qPCR array cards (#A34717, Life Technologies) for detection of up to 188 unique miRNAs in one serum/plasma sample. Endogenous and exogenous miRNA controls for normalization of data results are included in the array card. Data were collected at 0.1 threshold value on Applied Biosystems ViiA7 Real Time PCR System. The Ct values were normalized to the mean of Ct values of cel-mir-39 and analyzed with software Expression Suite (Life Technologies).

PUBLIC DATASETS AND BIOINFORMATIC ANALYSIS

Gene Expression Omnibus (GEO) GSE112264 dataset reporting serum miRNA profiles data in samples from 809 prostate cancers patients and 41 healthy control volunteers was analyzed using GEO2R software. Gene Expression Profiling Interactive Analysis (GEPIA) web server was used for expression analysis of COL271A gene in PCa (n=492) and normal tissue (n=152) from PCa patients and

healthy control volunteers from the Cancer Genome Atlas Prostate Adenocarcinoma (TCGA-PRAD) and Genotype-Tissue Expression (GTEx) datasets. DIANA-miRPath 3.0 web server tool (http://diana.cslab.ece.ntua.gr/pathways/) was used to perform the enrichment analysis of validated miRNA:gene interactions for each miRNA followed by targeted pathway analysis. miRNET free software was used to generate miRNA:gene interactions network (https://www.mirnet.ca/). Please, refer to data availability statement section for additional information.

STATISTICAL ANALYSIS

All data are presented as mean ± standard deviation (SD) unless stated otherwise. Statistical significance was determined by two-tailed Student's t-test. Statistical significance for multiple comparisons was calculated by using Kruskal-Wallis test. p-values of < 0.05 were considered statistically significant. Analyses used GraphPad Prism version 6.0 for Windows, GraphPad Software (San Diego, CA).

DRUG DELIVERY ANALYSIS

BD FACS Melody™ Cell Sorter was used to investigate the delivery of scramble (SCRB) D-tripeptide-FITC in DU145 cell line. After ultrasound treatment cells were rinsed twice with PBS, centrifuged at 4°C at 3000 rpm, resuspended in 500 µl of PBS, in polystyrene tubes, and analyzed. FACS analysis was performed with BD FACS Chorus™ Software.

RESULTS

ULTRASOUND TREATMENT INCREASES THE RELEASE OF KNOWN BIOMARKERS IN PROSTATE CANCER CELL LINES

A panel of AD (LNCaP, 22Rv1) and AI (DU145, PC3) PCa cell lines were analyzed for the expression of PSA biomarker by RT-qPCR. We found that LNCaP cells expressed the higher levels of PSA (fold change [FC]: 51679.64) compared to the other three cell lines, in which PSA expression was either significantly lower (22Rv1, FC: 196.98; PC3, FC: 3.08) or absent (DU145) (Figure 6A). As circulating PSA detection is routinely used in clinic for PCa screening, we tested if US treatment could improve the release of this biomarker in the supernatant of LNCaP and 22Rv1, the two cell lines where we detected measurable levels of PSA mRNA. To this end, both cell lines were treated with Promedica® Bioeletronics srl automatized prototype Sonowell®. The media was collected before and after the sonication from the same well to normalize biomarkers values on the same cells number; 10% of duty cycle was chosen to prevent membrane disruption and morphological alterations. Setting experiments identify 1 MHz frequency as the transducer that produced the more homogeneous sonication of the well, based on the cell area coverage analysis (Figure 6B). Supernatant PSA levels were detected by ELISA. After 30 minutes of US treatment, LNCaP cells released measurable levels of PSA in the supernatant, which were found to be almost tripled compared to those released by untreated control cells (FC: 2.87) (Figure 6C). Instead, we observed no difference in PSA release between US-treated 22Rv1 and untreated cells. As additional control of our system, we further tested our PCa cell lines for

the release, before and after US treatment, of three cell-free miRNAs previously isolated in LNCaP supernatants after US treatment: mir-16-5p, mir-141, mir-200c (D'Souza et al., 2018). The release of these selected miRNAs in the supernatant was evaluated through RT-qPCR after total miRNAs extraction. We found increased levels of mir-16-5p and mir-141 in both LNCaP (mir-16-5p, FC: 5.3; mir-141, FC: 2.8) and DU145 (mir-16-5p, FC: 13.6; mir-141, FC: 11.17) supernatant following US treatment, while an increased US-induced release of mir-200c was detected only in LNCaP supernatant (FC: 8.5). No significant increase of miRNA release was detected in PC3 and 22Rv1 supernatant after US treatment (Figure 6D-6F). The different response to US treatment observed across PCa cell lines could be due to their diverse morphology, which affects US-induced membrane permeability (Lentacker et al., 2014; Miller and Battaglia, 2003; Zhou et al., 2009). We concluded that US treatment is effective in increasing the extracellular release of PCa-related miRNAs, at least in some cellular settings.

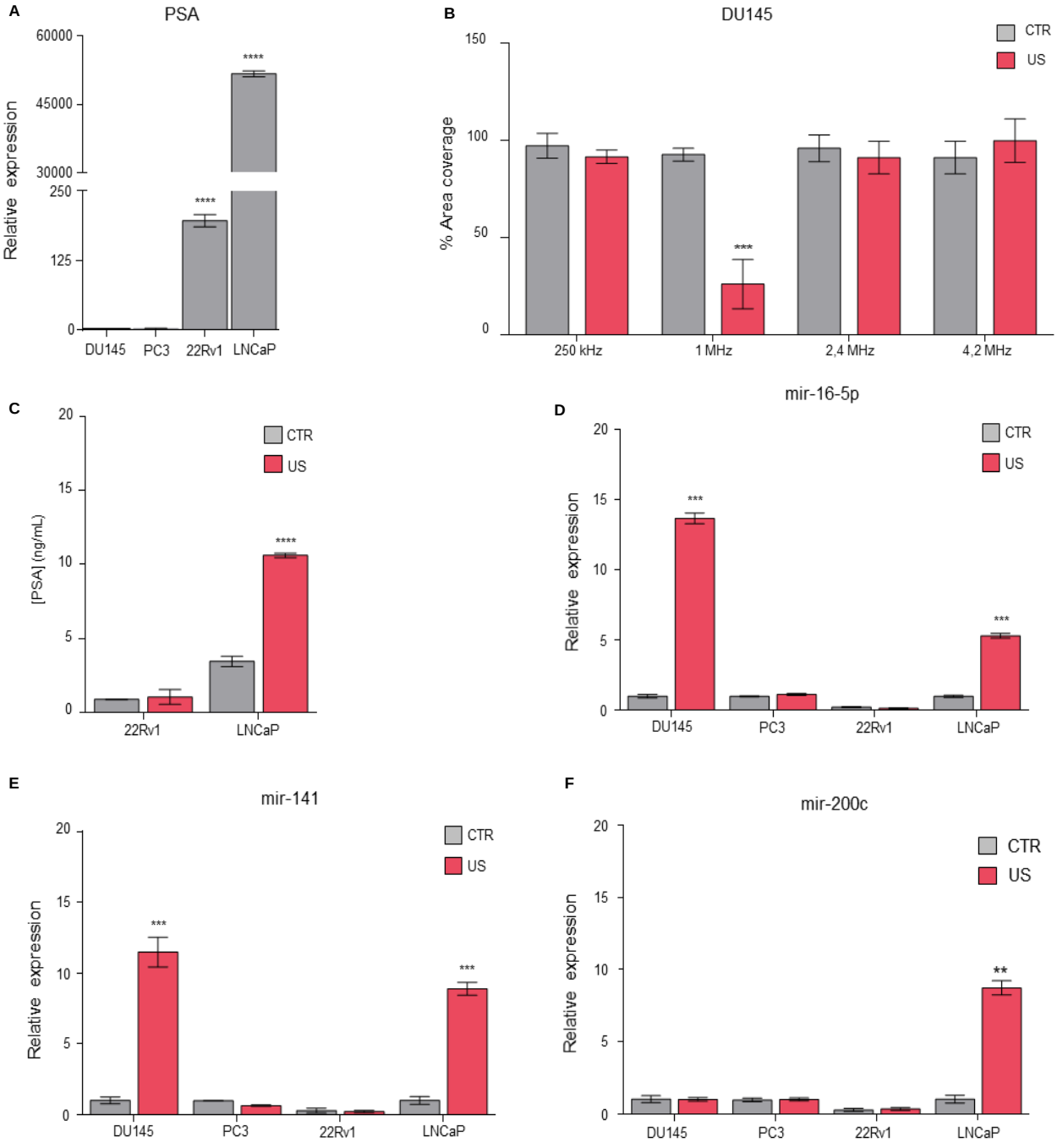

Figure 6. A, RT-qPCR showing PSA relative mRNA levels in the indicated PCa cell lines. **B**, ImageJ area coverage analysis showing the percentage of Crystal Violet-stained DU145 left in the well plate following US-treatment at maximum power using the indicated transducers. **C**, Quantification of PSA release in supernatant of untreated LNCaP and 22Rv1 (CTR) or US-treated cells. **D-F**, RT-qPCR showing levels of (D) mir-16-5p, (E) mir-141 and (F) mir-200c in DU145, PC3, 22Rv1 and LNCaP supernatant from US-treated cells relative to untreated control cells. A-F, Values denote means ± SD (n=3); statistical significance was calculated by two-tailed Student's t-test. **, $p<0.01$; ***, $p<0.001$; ****, $p<0.0001$

IDENTIFICATION OF NOVEL MICRORNA IN THE SUPERNATANT OF PROSTATE CANCER CELLS FOLLOWING US TREATMENT

Since US treatment showed to be effective in increasing the concentration of known miRNAs released in the supernatant of LNCaP and DU145 cells, we profiled miRNAs released by these cells before and after US treatment, with the aim of identifying new potential PCa-related miRNA biomarkers. The miRNA profile analysis was performed by TaqMan™ Advanced miRNA Human Serum/Plasma RT-qPCR array cards. The volcano plots in Figure 7 shows the log2FC of all miRNAs detected in LNCaP (Figure 7A) or DU145 (Figure 7B) supernatant after 1 hour US treatment compared to those released from untreated cells over the same time interval (Table 1). Among the 188 miRNAs investigated, we identified 4 miRNAs, whose levels were significantly higher in LNCaP cell supernatant after US treatment compared to those to those detected in basal conditions: miR-425-5p (FC: 5.129, p=0.028); miR-365b-3p (FC: 4.698, p=0.036); miR-629-5p (FC: 2.274, p=0.038), and miR-193b-3p (FC: 3.034, p=0.018). Three of them, miR-425-5p, miR-365a-3p and miR-193b-3p, were already described in the literature to be involved in PCa. In fact, miR-425-5p has been described to be overexpressed in prostate cancer cell lines, where it promotes proliferation, migration and invasion by targeting forkhead box J3 (Zhang et al., 2019); miR-365b-3p expression resulted statistically different in PCa tissues compared to those from patients with prostatic hyperplasia (Lyu et al., 2019); and miR-30b-5p was described to modulate NUAK1, whose alteration is required for prostate cancer progression (Guan et al., 2018). Interestingly, we also identified miR-629-5p, which to our knowledge had never been linked to PCa disease (Figure 7A, Table 1). Notably, two additional miRNAs, whose supernatant levels were increased more than two-fold following LNCaP US treatment - miR-374a-5p (FC: 2.550, p=0,060) and miR-194-5p (FC: 4.416,

p=0,195) – were not described in the literature as PCa-related miRNAs. DU145 profiling showed a significant increase in the release of let-7d-5p (FC:2.694, p=0.007) following US treatment and, although this miRNA family has been related to several cancer (Wagner et al., 2014), no specific roles in PCa have been described for this specific member (Figure 7B, Table 1). We investigated the cellular release kinetics of newly identified miR-629-5p, miR-374a-5p, miR-194-5p and let-7d-5p by single RT-qPCR assay. Release of miRNAs in the supernatant of LNCaP and DU145 was measured after treating cells with US for 15 minutes, 30 minutes and 1 hour. Supernatants of untreated control cells were collected before sonication, following incubation with exosomes-depleted medium for the same time. We observed a significant increase in the release of miR-629-5p, miR-374a-5p and miR-194-5p in LNCaP supernatant after 1h US treatment compared to untreated cells (miR-629-5p, FC: 6.5; miR-374a-5p, FC: 7.1; miR-194-5p, FC: 6.4), while no significant increase was observed at earlier time points (Figure 8A-C). Instead, we observed a time-dependent increase of let-7d-5p release in cell supernatant from US-treated DU145 cells compared to untreated cells. This increase in miRNA release was already significant after 15 minutes of US treatment (FC: 2.8) and augmented when cells were treated for longer time intervals (30’ treatment, FC: 40; 1h treatment, FC: 81.3) (Figure 8D).

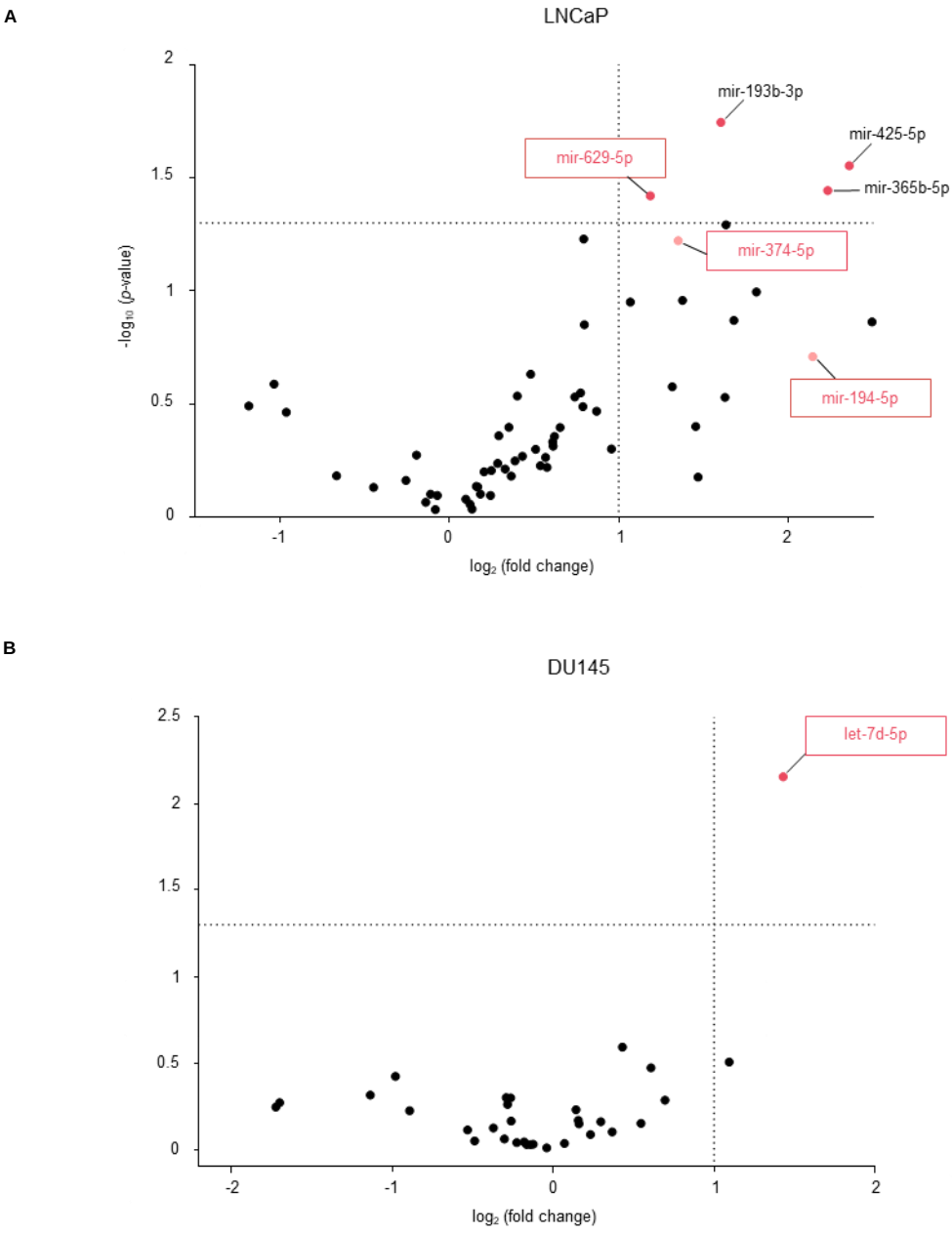

Figure 7. A-B, Volcano plots showing the profiling of released miRNAs in (A) LNCaP or (B) DU145 supernatant of US-treated relative to untreated control cells performed by using TaqMan™ Advanced miRNA Human Serum/Plasma Card RT-qPCR array cards. Analyses were performed using Expression Suite software. Reported are the negative log10 p-values plotted against the log2 fold change. Dots represent individual miRNAs. Horizontal line, p=0.05; Vertical line, FC=2. Dark red dots, significantly up-released miRNAs ($p<0.05$). miRNA of interested are depicted (framed boxes).

LNCaP			
microRNA	**Fold Change**	**Log2 Fold Change (US treated/untreated)**	**p-value**
hsa-miR-193b-3p-478314_mir*	3.034	1.60122109	0.018
hsa-miR-425-5p-478094_mir*	5.129	2.35867757	0.028
hsa-miR-365b-3p-478065_mir*	4.698	2.23204671	0.036
hsa-miR-629-5p-478183_mir*	2.274	1.18523225	0.038
hsa-miR-30b-5p-478007_mir	3.098	1.63133714	0.051
hsa-miR-374a-5p-478238_mir	2.55	1.35049725	0.060
hsa-miR-28-5p-478000_mir	2.096	1.06763872	0.112
hsa-miR-342-3p-478043_mir	2.595	1.37573454	0.110
hsa-miR-30c-5p-478008_mir	3.509	1.81105995	0.101
hsa-miR-99b-5p-478343_mir	5.627	2.49236596	0.137
hsa-miR-200c-3p-478351_mir	3.2	1.67807191	0.135
hsa-miR-194-5p-477956_mir	4.416	2.14274017	0.195
hsa-miR-148b-3p-477824_mir	2.488	1.31498649	0.265
hsa-miR-2110-477971_mir	3.086	1.62573806	0.295
hsa-miR-339-5p-478040_mir	2.739	1.45364927	0.397
hsa-miR-21-3p-477973_mir	2.764	1.46675762	0.664
hsa-miR-103a-3p-478253_mir	1.733	0.79327165	0.059
hsa-miR-374b-5p-478389_mir	1.737	0.79659775	0.141
hsa-miR-19a-3p-479228_mir	1.395	0.48026512	0.233
hsa-miR-182-5p-477935_mir	1.711	0.77483976	0.282
hsa-miR-195-5p-477957_mir	1.671	0.74071173	0.294
hsa-miR-500a-5p-478309_mir	1.727	0.78826808	0.324
hsa-miR-532-5p-478151_mir	1.826	0.86868677	0.34
hsa-miR-222-3p-477982_mir	1.941	0.95680012	0.499
hsa-miR-320e-478022_mir	1.573	0.65351867	0.401
hsa-miR-25-3p-477994_mir	1.538	0.6210555	0.439
hsa-miR-652-3p-478189_mir	1.526	0.60975496	0.464
hsa-miR-378a-3p-478349_mir	1.529	0.61258841	0.485
hsa-miR-132-3p-477900_mir	1.483	0.5685186	0.543
hsa-miR-221-3p-477981_mir	1.492	0.57724754	0.601
hsa-miR-125b-5p-477885_mir	1.452	0.53804145	0.591
hsa-miR-423-3p-478327_mir	1.424	0.50994915	0.5
hsa-miR-186-5p-477940_mir	1.349	0.43189035	0.537
hsa-miR-200a-3p-478490_mir	1.309	0.3884651	0.563
hsa-miR-34a-5p-478048_mir	1.288	0.36513259	0.657
hsa-miR-29a-3p-478587_mir	1.257	0.32998465	0.611
hsa-miR-93-5p-478210_mir	1.219	0.28569813	0.577
hsa-miR-19b-3p-478264_mir	1.225	0.29278175	0.436
hsa-miR-191-5p-477952_mir	1.276	0.35162833	0.4
hsa-miR-92a-3p-477827_mir	1.321	0.40163047	0.291

hsa-miR-26b-5p-478418_mir	1.188	0.24853484	0.621
hsa-miR-26a-5p-477995_mir	1.153	0.20539251	0.629
hsa-miR-21-5p-477975_mir	1.117	0.15962919	0.729
hsa-miR-20a-5p-478586_mir	1.124	0.16864204	0.733
hsa-miR-29b-3p-478369_mir	1.136	0.18396283	0.79
hsa-miR-484-478308_mir	1.184	0.24366908	0.8
hsa-miR-17-5p-478447_mir	1.07	0.0976108	0.831
hsa-miR-28-3p-477999_mir	1.088	0.12167856	0.873
hsa-miR-125b-5p-477885_mir	1.098	0.13487805	0.918
hsa-miR-301a-3p-477815_mir	0.953	-0.0694519	0.8
hsa-let-7g-5p-478580_mir	0.927	-0.1093588	0.789
hsa-miR-339-3p-478325_mir	0.909	-0.1376478	0.857
hsa-miR-190a-5p-478358_mir	0.945	-0.0816138	0.923
hsa-miR-148a-3p-477814_mir	0.875	-0.1926451	0.531
hsa-miR-24-3p-477992_mir	0.838	-0.2549779	0.686
hsa-miR-324-5p-478024_mir	0.734	-0.446148	0.737
hsa-miR-151a-3p-477919_mir	0.631	-0.6642881	0.655
hsa-miR-505-3p-478145_mir	0.514	-0.9601597	0.343
hsa-miR-130b-3p-477840_mir	0.489	-1.0320936	0.258
hsa-miR-210-3p-477970_mir	0.441	-1.1811494	0.322
DU145			
microRNA	**FC**	**Log2 FC**	**p-value**
hsa-let-7d-5p-478575_mir*	2.694	1.42974985	0.007
hsa-miR-191-5p-477952_mir	2.135	1.09423607	0.312
hsa-miR-21-5p-477975_mir	1.348	0.4308205	0.256
hsa-miR-24-3p-477992_mir	1.525	0.60880924	0.337
hsa-miR-342-3p-478043_mir	1.62	0.69599381	0.518
hsa-miR-23a-3p-478532_mir	1.46	0.54596837	0.706
hsa-miR-151a-3p-477919_mir	1.29	0.36737107	0.791
hsa-miR-15a-5p-477858_mir	1.228	0.29631056	0.691
hsa-miR-10a-5p-479241_mir	1.175	0.23266076	0.819
hsa-miR-31-5p-478015_mir	1.118	0.16092019	0.71
hsa-miR-29b-3p-478369_mir	1.115	0.15704371	0.678
hsa-miR-93-5p-478210_mir	1.104	0.14274017	0.589
hsa-miR-26a-5p-477995_mir	1.05	0.07038933	0.922
hsa-miR-99b-5p-478343_mir	0.973	-0.0394883	0.978
hsa-miR-652-3p-478189_mir	0.918	-0.1234339	0.932
hsa-miR-155-5p-477927_mir	0.907	-0.1408255	0.935
hsa-miR-181a-5p-477857_mir	0.892	-0.1648844	0.936
hsa-miR-222-3p-477982_mir	0.883	-0.1795147	0.903
hsa-miR-25-3p-477994_mir	0.855	-0.2260037	0.912
hsa-miR-320a-478594_mir	0.811	-0.3022262	0.868
hsa-miR-423-3p-478327_mir	0.835	-0.2601519	0.684

hsa-let-7g-5p-478580_mir	0.822	-0.2827897	0.549
hsa-miR-125b-5p-477885_mir	0.833	-0.2636116	0.503
hsa-miR-29a-3p-478587_mir	0.817	-0.291592	0.501
hsa-miR-186-5p-477940_mir	0.773	-0.3714597	0.751
hsa-miR-532-5p-478151_mir	0.713	-0.488026	0.893
hsa-miR-200c-3p-478351_mir	0.692	-0.5311561	0.77
hsa-miR-193b-3p-478314_mir	0.539	-0.8916428	0.597
hsa-miR-221-3p-477981_mir	0.507	-0.9799423	0.378
hsa-miR-502-3p-478348_mir	0.455	-1.1360615	0.485
hsa-miR-28-3p-477999_mir	0.308	-1.6989977	0.536
hsa-miR-500a-5p-478309_mir	0.303	-1.7226103	0.568

Table 1. Cell-free miRNAs profiling of US-treated LNCaP and DU145 cells. Significantly up-released miRNAs, $p < 0$.

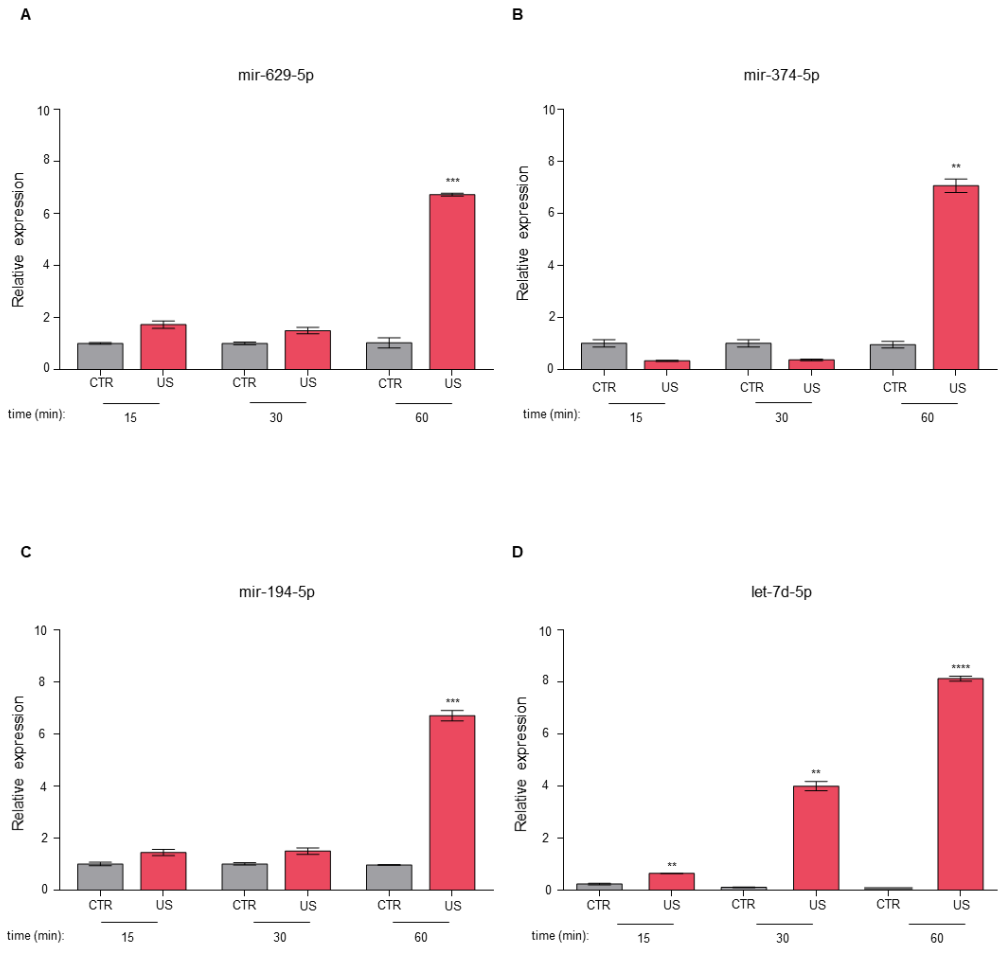

Figure 8. A-C, Single RT-qPCR assay showing cellular release kinetics of (A) mir-629-5p, (B) mir-374-5p and (C) mir-194-5p in LNCaP supernatants following US treatment for different time periods. **D**, Single RT-qPCR assay showing cellular release kinetics of let-7d-5p in DU145 supernatants following US treatment for different time periods. **A-D**, Expression values are relative to untreated control cell. Values denote means ± SD (n=3); statistical significance was calculated by two-tailed Student's t-test. **, $p<0.01$; ***, $p<0.001$; ****, $p<0.0001$.

NEWLY IDENTIFIED MICRORNAS ARE UPREGULATED IN SERUM FROM PROSTATE CANCER PATIENTS

To understand the clinical significance of these four miRNAs identified in PCa cell supernatants following US treatment, we analyzed their expression in serum from non-cancer controls (n=41) or PCa patients (n=809) from the GSE112264 publicly available dataset. This analysis showed that serum expression of all miRNAs was significantly upregulated in PCa patients compared to controls (Figure 9A-9D), suggesting that they could be potential valuable diagnostic biomarkers. We also analyzed serum expression of these miRNAs in PCa patients stratified based on tumor stage. mir-629-5p, mir-374-5p and mir-194-5p expression levels were increased in serum of PCa patients across all tumor stages compared to control sera (Figure 10A-10C), while let-7d-5p mRNA levels were significantly higher only in serum from patients with T1-T3 PCa disease (Figure 10D). Thus, all analyzed miRNAs seem to be released in serum of PCa patients in the earlier phases of disease (T1-T2 stages), and their levels remain high as the disease progresses to advanced stages (T3-T4 stages).

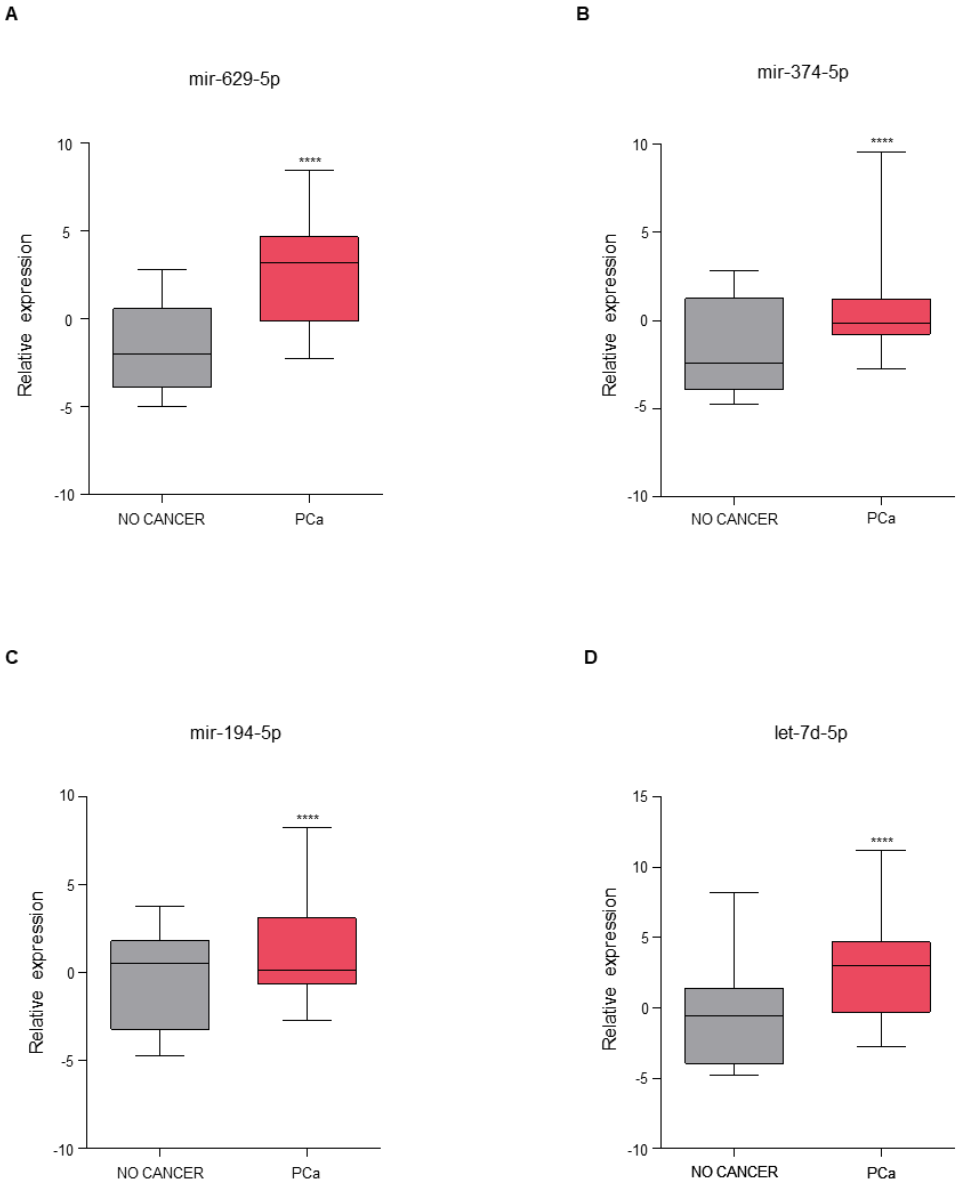

Figure 9. A-D, Boxplot showing expression of (A) mir-629-5p, (B) mir-374-5p, (C) mir-194-5p and (D) let-7d-5p in serum from control healthy volunteer (n=41) or human PCa patients (n=809) from GSE112264 dataset. Shown in the boxplot are the medians (horizontal lines), 25th-75th percentiles (box outlines), and highest and lowest values within 1.5x of the inter-quartile range (vertical lines). Statistical significance was calculated by using two-tailed Student's t-test. ****, p-value < 0.0001.

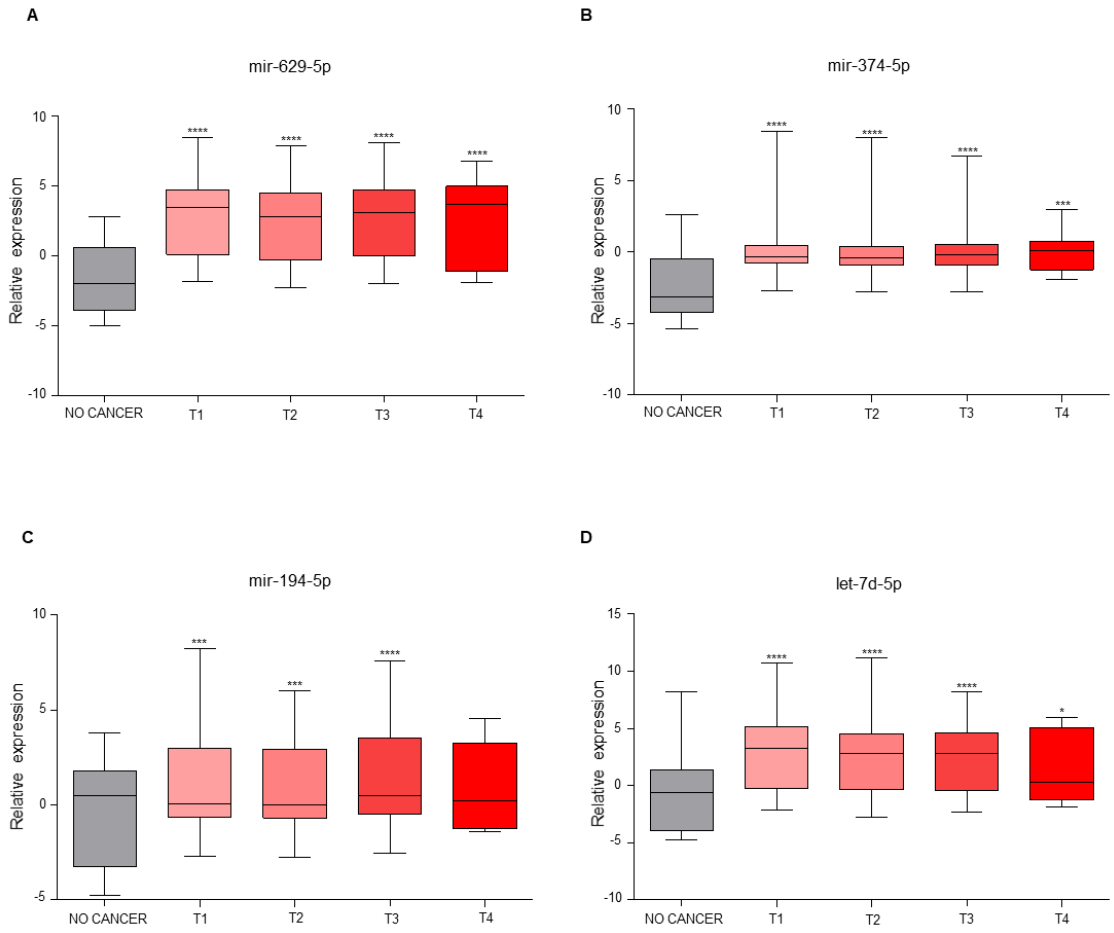

Figure 10. A-D, Boxplot showing expression of (A) mir-629-5p, (B) mir-374-5p, (C) mir-194-5p and (D) let-7d-5p in serum from control healthy volunteer (n=41) or human PCa patients from GSE112264 dataset stratified for tumour staging (T1=256 samples, T2=354 samples, T3=183 samples, T4 stage=16 samples). Shown in the boxplot are the medians (horizontal lines), 25th-75th percentiles (box outlines), and highest and lowest values within 1.5x of the inter-quartile range (vertical lines). Samples from each tumour stage was compared to control healthy group by using two-tailed Student's t-test. *, p-value < 0.05; ***, p-value < 0.001; ****, p-value < 0,0001. Statistical significance for multiple comparisons was calculated by using Kruskal-Wallis test. A-B, D, p-value < 0,0001; C, p-value = 0.0146.

IN SILICO MICRORNA: GENE INTERACTION ANALYSIS

In order to better characterize the newly PCa-related miRNAs, we conducted an in-silico analysis to identify the biological targets of mir-629-5p, mir-374-5p, mir-194-5p and let-7d-5p, with the aim of defining their roles in PCa development and progression. To this end, DIANA-mirPath 3.0 was used to search out both experimentally validated and putative target genes, by exploiting two different bioinformatic tools: *i)* TarBase v7.0, which shows gene targets validated in high throughput, microarrays, sequencing and proteomic experiments; and *ii)* microT-CDS, which identifies putative target genes by using an algorithm based on the recognition of positive and negative sets of miRNA Recognition Elements (MREs) located in both the 3'-UTR and CDS regions. Enrichment analysis of validated miRNA:gene interactions followed by targeted pathway analysis (Table 2, Figure 11A) showed that both mir-629-5p and miR-194-5p target DHCR24 gene, a central regulator of steroid biosynthesis, which is frequently altered in prostate cancer cells (Battista et al., 2010). Among the validated gene targets of both miR-194-5p and miR-374a-5p we also found CCND2, AXIN2 and BMPR2, regulated by the Hippo signaling pathway involved in stemness and cancer biology. miR-374a-5p seems also to be involved in the regulation of biosynthesis of unsaturated fatty acids by targeting genes like ELOVL5, SCD and HSD17B12, thus reinforcing the well-known correlation between altered lipid metabolism and prostate cancer (Centenera et al., 2021; Kim et al., 2011; Sun et al., 2011). Both miR-374a-5p and let-7d-5p target several genes previously associated with the KEGG prostate cancer pathway. Moreover, we found that let-7d-5p, identified in the supernatant of DU145 following US treatment, regulated genes involved in glioma-associated KEGG pathway, and this is of interest as DU145 were isolated from brain metastasis of PCa. Indeed, these two KEGG pathways shares many genes, like CCND1, which

plays a fundamental role in the regulation of cell cycle and proliferation in both glioma and prostate cancer cells, and whose deregulation portends worse clinical outcomes (Chung et al., 2019; Ikeda et al., 2019). let-7d-5p also modulated genes implicated in cell-cell adherens junctions, suggesting a role for this miRNA in regulating the epithelial mesenchymal transition (EMT), a process promoting PCa metastasis and chemoresistance (Sowalsky et al., 2015). In addition to validated gene interactors, we searched for putative target genes of our miRNAs of interest. Enrichment analysis of putative miRNA:gene interactions followed by targeted pathway analysis performed by microT-CDS suggested that miR-629-5p could also target the prolactin receptor (PRLR) and AKT serine/threonine kinase 3 (AKT3) genes, involved in the prolactin signaling pathway, whose alteration may contribute to the pathogenesis of PCa (Table 2) (Lin et al., 2015; O'Sullivan and Bates, 2016). The same analysis showed that miR-194-5p could be also involved in the regulation of branched chain amino acid degradation, a metabolic process found deregulated in PCa progression (Table 2) (Zhu et al., 2017). Interestingly, among putative targets for let-7d-5p, we found that COL27A1, codifying for fibrillar collagen alpha-1 (XXVII) chain protein and to our knowledge never associated with PCa, was the only one downregulated in PCa patients from The Cancer Genome Atlas (TCGA) compared to controls, suggesting a potential role for this let-7d-5p-target gene in PCa pathogenesis (Table 2, Figure 11B) (Pace et al., 2003).

miRNAs	**miR-629-5p**	**miR-374a-5p**			**miR-194-5p**		**let-7d-5p**		
KEGG pathways	Steroid biosynthesis	UFA biosynthesis	Hippo pathway	Prostate cancer	Hippo pathway	Steroid biosynthesis	Adherens junction	Glioma	Prostate cancer
***p*-value**	4.63E-05	3.08E-08	3.085E-08	2.21E-02	2.65E-04	5.30E-04	1.94E-06	8.64E-03	2.37E-02
Target Genes	DHCR24	ELOVL5 SCD HSD17B12	GSK3B YAP1 APC NF2 WNT5A CCND2 FZD6 WNT3 YWHAB WWTR1 FZD3 MPP5 CCND1 CTNNB1 CTNNA1 FRMD6 TEAD1 LATS1 FBXW11 PPP2R1B PARD6B BMPR2 PPP1CB	NRAS PIK3CB CDKN1B IGF1R KRAS CCND1 CTNNB1 CCNE2 PDGFC CREB3L2 PTEN MAPK1 MDM2	TGFBR1 YAP1 YWHAE CCND2 ACTG1 CCND1 AXIN2 BMPR2	DHCR24	ACTB CSNK2A2 TGFBR1 WASF1 SMAD2 ACTG1 SMAD3 IGF1R VCL TJP1 FYN ACP1 NLK PTPN6 WASF2 FER CSNK2A1 FARP2 PTPRJ RAC1 INSR FGFR1 MAPK1 CREBBP TGFBR2	BRAF CDK4 E2F2 NRAS IGF1R TP53 PLCG1 CCND1 E2F3 PDGFB CDKN1A MTOR MAPK1 MDM2	BRAF E2F2 NRAS HSP90AA1 IGF1R TP53 AR CCND1 CCNE2 E2F3 PDGFB CDKN1A MTOR FGFR1 MAPK1 CREBBP MDM2

Table 2. Enrichment analysis of putative miRNA:gene interactions followed by targeted pathway analysis.

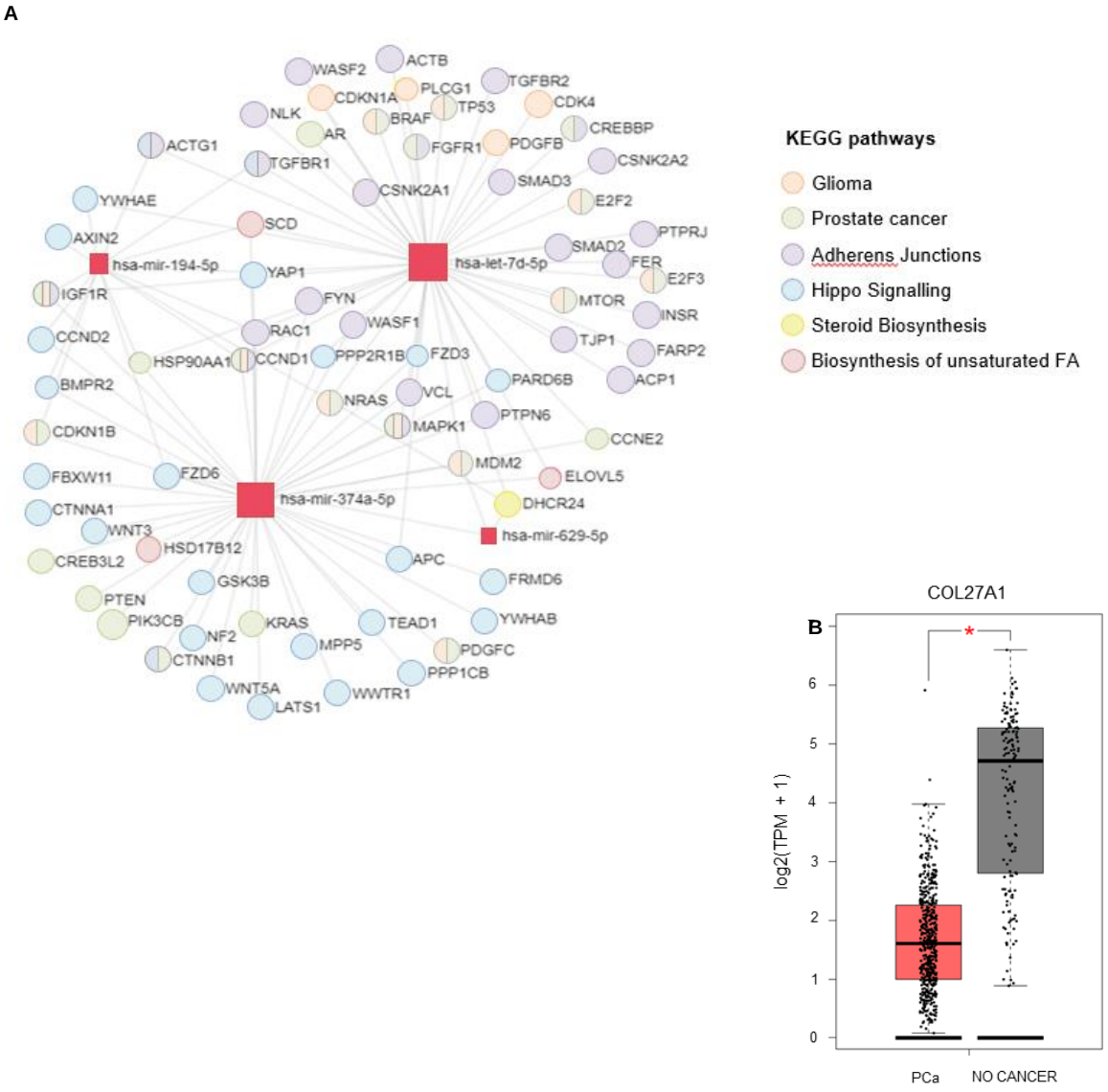

Figure 11. A, Schematic representation of miRNA:gene network resulting from enrichment analysis of validated miRNA:gene interactions followed by targeted pathway analysis. A colour code was used for grouping genes from the same KEGGS pathway. **B**, Boxplots showing the mRNA expression of COL27A1 in tumour samples of PCa (n=492) from PRAD-TCGA dataset and normal tissue (n=152) from TCGA and Genotype-Tissue Expression (GTEx) datasets. Expression analysis was performed by using Gene Expression Profiling Interactive Analysis (GEPIA) web server. Statistical significance was calculated by one-way ANOVA. TPM, transcripts per million. **A-B,** p-value < 0.05.

ULTRASOUND-MEDIATED DRUG DELIVERY

The delivery of a SCRB D-tripeptide-FITC on DU145 cells in presence of two different ultrasound regimens (1MHz, DC 10%, Ispta 410.5 mW/cm^2, 500 kPa for 3 sec, 30sec, 60 sec and 1MHz, DC 10%, Ispta 307.9 mW/cm^2, 250 kPa, for 180 sec, 300s, 600 sec) was evaluated by FACS. The short time higher-pressure treatment, generating 500 kPa inside the well, enhanced the delivery of the SCRB-FITC in inversely proportional manner with the time of sonication. The percentage of cells FITC-positivity ranged from 70,86% after 3 sec of treatment to 60,61% after 30 sec and to 58,72% after 60 sec of sonication (Figure 12, middle panel). Following the lower-pressure treatment we observed a less efficient drug delivery that seemed to slightly increase in a time dependent manner, with the FITC-positivity ranging from 7,92% at 180 sec, 9,65% at 300 sec and 13,88% at 600 sec (Figure 12, bottom panel). Both ultrasound regimens facilitated the delivery of SCRB-FITC respect to control cells, which were incubated in basal conditions with conjugated molecules for the maximum time of treatment (*i.e.*, 600 sec) (Figure 12, upper panel).

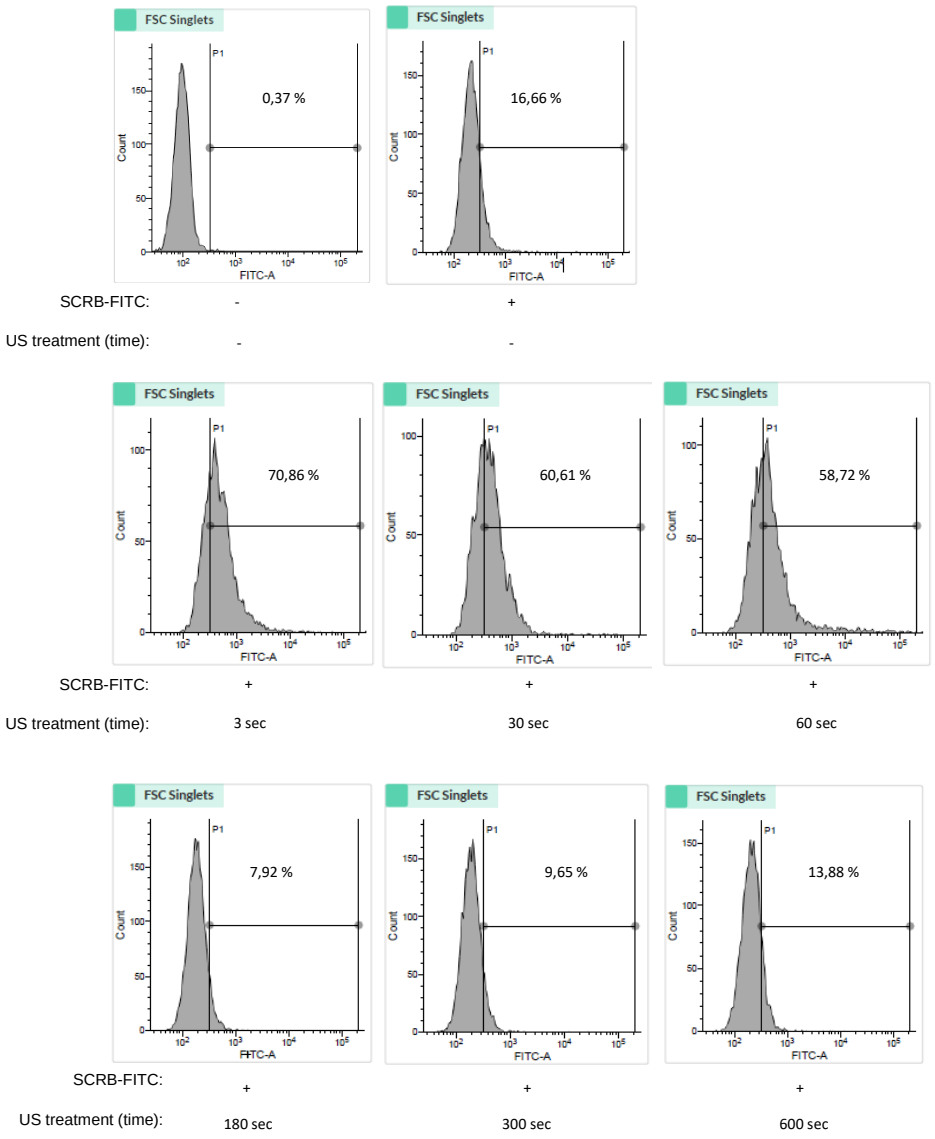

Figure 12. A-C, FACS analysis of SCRB-FITC delivery in DU145 after ultrasound treatment. **A-B**, Time course delivery of SCRB-FITC molecules following short time higher-pressure treatment (A) and lower-pressure treatment (B). Percentage of FITC-positivity and time of treatment are depicted. **C**, Percentage of FITC-positivity in control cells incubated in basal conditions and with conjugated molecules, for the maximum time of treatment.

DISCUSSION

The use of circulating miRNA biomarkers for improving cancer diagnosis and monitoring treatment response is showing promise for clinical utility (Kishikawa et al., 2015). However, they are often present at or below quantifiable limits, especially at early-stage disease (Witwer, 2015). Our study provided evidence that US-mediated sonoporation could be a powerful tool to amplify the release of prognostic miRNAs from both AD and AI PCa cells, in keeping with recent studies showing an increased release of known PCa-related miRNA biomarkers from LNCaP cells (D'Souza et al., 2018). Notably, preliminary data in rat allografts and patients with uterine fibroids showed that US treatment could be effective in stimulating the release of intracellular biomarkers in body fluids, suggesting that this technique could be clinically useful for earlier detection of cancer lesions (Chevillet et al., 2017; D'Souza et al., 2018).

Due to the low predictive value of current detection and prognostication tools, PCa overdiagnosis and overtreatment remains a major challenge. Although several studies identified many miRNAs involved in PCa development and progression and investigated their potential as PCa non-invasive biomarkers for early diagnosis and prediction of metastasis (Bidarra et al., 2019; Haldrup et al., 2014), validation of multiple biomarkers is crucial for an effective detection and management of cancer disease (Kelly et al., 2015; Radon et al., 2015). Interestingly, in this regard, our miRNA profiling of US-treated cell supernatants allowed the identification of four novel PCa-related miRNAs with potential diagnostic and predictive value: mir-629-5p, mir-374-5p, mir-194-5p and let-7d-5. Indeed, our results showed that their expression in sera from PCa patients is higher compared to their levels in sera from

healthy volunteer. Moreover, we showed that these miRNAs seem to be released in the earlier phases of disease, and their levels remain high as the disease progresses to advanced stages, suggesting that they might be valuable tools to improve early cancer detection and patient management along with the currently used biomarkers.

Furthermore, our analysis of miRNA: gene interactions showed that they target many well-known PCa-related genes, which are often downregulated in aggressive PCa. Indeed, reduced expression of DHCR24, a target of both mir-629-5p and miR-194-5, just like other AR-related genes, correlates with prostate cancer progression and higher risk to develop metastases in primary PCa specimens, since the androgens induce differentiation and inhibit the growth of prostate epithelial cells (Bonaccorsi et al., 2008). Downregulation of CCND2, AXIN2 and BMPR2, targeted by miR-194-5p and miR-374a-5p, were also associated with advanced PCa disease. In particular, CCND2 reduced expression was found in more aggressive prostate tumors characterized by high Gleason score and elevated PSA levels, suggesting that it could be an indicator of increased risk of relapse (Chen et al., 2017), while downregulation of AXIN2 and BMPR2 was associated with high tumor grade, invasiveness and recurrence (Dai et al., 2019; Kim et al., 2004) In addition to provide biological connection between newly identified miRNA and genes with a well described role in PCa biology, we also identified COLA27A1 as a putative target gene of let-7d-5p. We found that COLA27A1 mRNA expression is lower in PCa tumors compared to normal tissues, suggesting a potential role for this gene in PCa pathogenesis. Clinical studies suggested that tumor collagen content, alignment and distribution are prognostic factors in different cancers and specific chains of these collagens modulates key processes in cancer progression, acting as either pro- or anti-tumorigenic factor (Brisson et al., 2015; Chintala et al., 1996; Mammoto et al., 2013; Matte et al., 2019; Thangavelu et al., 2016).

Moreover, a recent study reported that low expression levels of COL27A1 were associated with a worse prognosis in breast cancer, pancreatic ductal adenocarcinoma and kidney renal clear cell carcinoma (Bourgot et al., 2020). Further investigations will determine the precise role of this gene in PCa progression.

We also demonstrated the applicability of the ultrasound treatment performed with Sonowell® platform in experiments of drug delivery, in which two different regimens of sonication were applied: a short-time higher-pressure treatment and a long-time lower-pressure treatment. The ultrasound regimen generating the higher pressure inside the well was the more efficient in inducing the delivery of the SCRB-FITC molecule in DU145 cells, with a 71% of FITC-positive cells detected after only 3 seconds of sonication. Interestingly, the delivery rate increased inversely with the time of sonication. An opposite behavior was observed following the long-time lower-pressure treatment, after which the percentage of FITC-positive cells was not only significantly reduced with respect to the other regimen, but it slightly increased with the time of sonication. Our results are consistent with previous studies that showed how at higher ultrasound intensities gas microbubbles (MB), normally present in medium, tend to behave non-linearly with their phases of compression and expansion until MB reach their resonant size. This behavior, also called “stable cavitation” or “non-inertial cavitation”, generated with pressure up to 1000 Pa, causes the oscillation of microbubbles that create a liquid flow, or microstreams, around the cells (Lentacker et al., 2014). Stable cavitation enables the transport of membrane impermeant compounds into the cytoplasm of cells through both an enhanced formation of pores and endocytosis (Meijering et al., 2009). On the other hand, at very low acoustic pressures, microbubbles oscillate in a linear and symmetrical way with a gas influx (during expansion) and gas efflux

(during compression) cycle netto equal to zero, thus reducing the biological effects induced by ultrasound (Quaia, 2005). This evidence could explain the differences we observed in SCRB-FITC delivery with the two US regimens. However, further studies are necessary to better explore drug retention when the delivery is mediated by US treatment and to understand if drug therapeutic efficacy is preserved once the molecules are delivered inside the cytoplasm.

In conclusion, our findings highlight the potential of using US to identify novel free-cell miRNAs released from cancer cells. The identification of new PCa-related cell-free miRNA may be crucial not only for the development of novel biomarkers but also to uncover novel potential pathogenetic mechanisms involved in PCa biology (Figure 13). Moreover, US treatment could be a useful tool to enhance drug delivery, especially when the physical and chemical characteristics of the molecules like molecular weight, size and charges of surface reduce or completely prevent the normal drug uptake from cells.

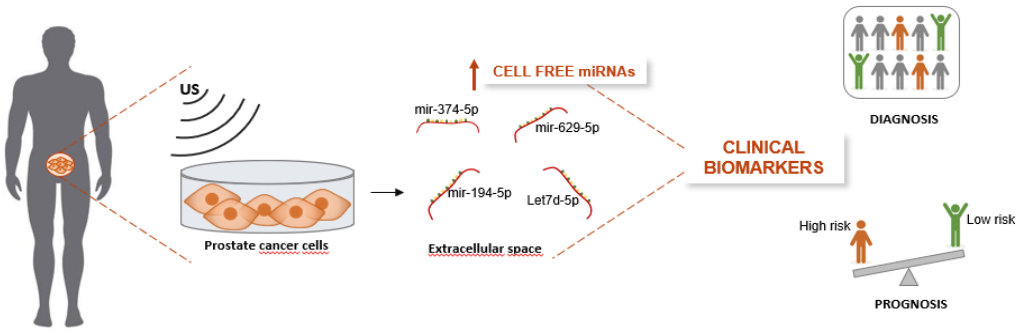

Figure 13. Graphical representation of the clinical application of novel microRNAs identified in the in-vitro model of prostate cancer after ultrasound treatment.

REFERENCES

Abdulkadir, S. A., Magee, J. A., Peters, T. J., Kaleem, Z., Naughton, C. K., Humphrey, P. A. and Milbrandt, J.: Conditional Loss of Nkx3.1 in Adult Mice Induces Prostatic Intraepithelial Neoplasia, Mol. Cell. Biol., 22(5), 1495–1503, doi:10.1128/MCB.22.5.1495-1503.2002, 2002.

Afadzi, M., Strand, S. P., Nilssen, E. A., Måsøy, S.-E., Johansen, T. F., Hansen, R., Angelsen, B. A. and de L Davies, C.: Mechanisms of the ultrasound-mediated intracellular delivery of liposomes and dextrans., IEEE Trans. Ultrason. Ferroelectr. Freq. Control, 60(1), 21–33, doi:10.1109/TUFFC.2013.2534, 2013.

Ammirante, M., Luo, J.-L., Grivennikov, S., Nedospasov, S. and Karin, M.: B-cell-derived lymphotoxin promotes castration-resistant prostate cancer., Nature, 464(7286), 302–305, doi:10.1038/nature08782, 2010.

Ando, H., Feril, L. B. J., Kondo, T., Tabuchi, Y., Ogawa, R., Zhao, Q.-L., Cui, Z.-G., Umemura, S.-I., Yoshikawa, H. and Misaki, T.: An echo-contrast agent, Levovist, lowers the ultrasound intensity required to induce apoptosis of human leukemia cells., Cancer Lett., 242(1), 37–45, doi:10.1016/j.canlet.2005.10.032, 2006.

Auprich, M., Bjartell, A., Chun, F. K.-H., de la Taille, A., Freedland, S. J., Haese, A., Schalken, J., Stenzl, A., Tombal, B. and van der Poel, H.: Contemporary role of prostate cancer antigen 3 in the management of prostate cancer., Eur. Urol., 60(5), 1045–1054, doi:10.1016/j.eururo.2011.08.003, 2011.

Ayala, A. G. and Ro, J. Y.: Prostatic intraepithelial neoplasia: recent advances., Arch. Pathol. Lab. Med., 131(8), 1257–1266, doi:10.1043/1543-2165(2007)131[1257:PINRA]2.0.CO;2, 2007.

Bandini, M., Gandaglia, G. and Briganti, A.: Obesity and prostate cancer., Curr. Opin. Urol., 27(5),

415–421, doi:10.1097/MOU.0000000000000424, 2017.

Belur, L. R., Podetz-Pedersen, K. M., Sorenson, B. S., Hsu, A. H., Parker, J. B., Carlson, C. S., Saltzman, D. A., Ramakrishnan, S. and McIvor, R. S.: Inhibition of angiogenesis and suppression of colorectal cancer metastatic to the liver using the Sleeping Beauty Transposon System., Mol. Cancer, 10(1), 14, doi:10.1186/1476-4598-10-14, 2011.

Bernstein, E., Kim, S. Y., Carmell, M. A., Murchison, E. P., Alcorn, H., Li, M. Z., Mills, A. A., Elledge, S. J., Anderson, K. V and Hannon, G. J.: Dicer is essential for mouse development., Nat. Genet., 35(3), 215–217, doi:10.1038/ng1253, 2003.

Bethel, C. R., Faith, D., Li, X., Guan, B., Hicks, J. L., Lan, F., Jenkins, R. B., Bieberich, C. J. and De Marzo, A. M.: Decreased NKX3.1 Protein Expression in Focal Prostatic Atrophy, Prostatic Intraepithelial Neoplasia, and Adenocarcinoma: Association with Gleason Score and Chromosome 8p Deletion, , doi:10.1158/0008-5472.CAN-06-0963, 2006.

Bidarra, D., Constâncio, V., Barros-Silva, D., Ramalho-Carvalho, J., Moreira-Barbosa, C., Antunes, L., Maurício, J., Oliveira, J., Henrique, R. and Jerónimo, C.: Circulating MicroRNAs as Biomarkers for Prostate Cancer Detection and Metastasis Development Prediction., Front. Oncol., 9, 900, doi:10.3389/fonc.2019.00900, 2019.

Bonaccorsi, L., Luciani, P., Nesi, G., Mannucci, E., Deledda, C., Dichiara, F., Paglierani, M., Rosati, F., Masieri, L., Serni, S., Carini, M., Proietti-Pannunzi, L., Monti, S., Forti, G., Danza, G., Serio, M., Peri, A., Chen, Y. Y., Zhang, Q., Wang, Q., Li, J., Sipeky, C., Xia, J., Gao, P., Hu, Y., Zhang, H., Yang, X., Chen, H., Jiang, Y., Yang, Y., Yao, Z., Chen, Y. Y., Gao, Y., Tan, A., Liao, M., Schleutker, J., Xu, J., Sun, Y., Wei, G.-H., Mo, Z., Fan, Z., Liu, H., Mayer, M., Deng, C. X., Zhou, Y., Kumon, R. E., Cui, J., Deng, C. X., Miller, M. W., Battaglia, L. F., Schneider, C. A., Rasband, W. S., Eliceiri, K. W., Lentacker, I., De Cock, I., Deckers, R., De Smedt, S. C., Moonen, C. T. W., Haldrup, C., Kosaka, N., Ochiya, T., Borre, M., Høyer, S., Orntoft, T. F., Sorensen, K. D.,

Cheng, H. H., Mitchell, P. S., Kroh, E. M., Dowell, A. E., Chéry, L., Siddiqui, J., Nelson, P. S., Vessella, R. L., Knudsen, B. S., Chinnaiyan, A. M., Pienta, K. J., Morrissey, C., Tewari, M., Bryant, R. J., Pawlowski, T., Catto, J. W. F., Marsden, G., Vessella, R. L., Rhees, B., Kuslich, C., Visakorpi, T., Hamdy, F. C., Wen, Y.-H., Chang, P.-Y., Hsu, C.-M., Wang, H.-Y., Chiu, C.-T., Lu, J.-J., Lin, H.-P., Lin, C.-Y., Huo, C., Jan, Y.-J., Tseng, J.-C., Jiang, S. S., et al.: The natural and treated history of prostate cancer, edited by H. Hricak and P. Scardino, Proc. Natl. Acad. Sci. U. S. A., 21(1), 15–28, doi:10.1017/CBO9780511551994.004, 2015.

Brase, J. C., Johannes, M., Schlomm, T., Fälth, M., Haese, A., Steuber, T., Beissbarth, T., Kuner, R. and Sültmann, H.: Circulating miRNAs are correlated with tumor progression in prostate cancer., Int. J. cancer, 128(3), 608–616, doi:10.1002/ijc.25376, 2011.

Bryant, R. J., Pawlowski, T., Catto, J. W. F., Marsden, G., Vessella, R. L., Rhees, B., Kuslich, C., Visakorpi, T. and Hamdy, F. C.: Changes in circulating microRNA levels associated with prostate cancer., Br. J. Cancer, 106(4), 768–774, doi:10.1038/bjc.2011.595, 2012.

Bussemakers, M. J., van Bokhoven, A., Verhaegh, G. W., Smit, F. P., Karthaus, H. F., Schalken, J. A., Debruyne, F. M., Ru, N. and Isaacs, W. B.: DD3: a new prostate-specific gene, highly overexpressed in prostate cancer., Cancer Res., 59(23), 5975–5979, 1999.

Califf, R. M.: Biomarker definitions and their applications., Exp. Biol. Med. (Maywood)., 243(3), 213–221, doi:10.1177/1535370217750088, 2018.

Calin, G. A. and Croce, C. M.: MicroRNAs and chromosomal abnormalities in cancer cells., Oncogene, 25(46), 6202–6210, doi:10.1038/sj.onc.1209910, 2006.

Cary, K. C. and Cooperberg, M. R.: Biomarkers in prostate cancer surveillance and screening: past, present, and future., Ther. Adv. Urol., 5(6), 318–329, doi:10.1177/1756287213495915, 2013.

Catalona, W. J., Partin, A. W., Slawin, K. M., Brawer, M. K., Flanigan, R. C., Patel, A., Richie, J. P., deKernion, J. B., Walsh, P. C., Scardino, P. T., Lange, P. H., Subong, E. N., Parson, R. E.,

Gasior, G. H., Loveland, K. G. and Southwick, P. C.: Use of the percentage of free prostate-specific antigen to enhance differentiation of prostate cancer from benign prostatic disease: a prospective multicenter clinical trial., JAMA, 279(19), 1542–1547, doi:10.1001/jama.279.19.1542, 1998.

Chandrasekaran, K., Karolina, D. S., Sepramaniam, S., Armugam, A., Wintour, E. M., Bertram, J. F. and Jeyaseelan, K.: Role of microRNAs in kidney homeostasis and disease., Kidney Int., 81(7), 617–627, doi:10.1038/ki.2011.448, 2012.

Chang, T.-C., Yu, D., Lee, Y.-S., Wentzel, E. A., Arking, D. E., West, K. M., Dang, C. V, Thomas-Tikhonenko, A. and Mendell, J. T.: Widespread microRNA repression by Myc contributes to tumorigenesis., Nat. Genet., 40(1), 43–50, doi:10.1038/ng.2007.30, 2008.

Chen, Y., Clegg, N. J. and Scher, H. I.: Anti-androgens and androgen-depleting therapies in prostate cancer: new agents for an established target., Lancet. Oncol., 10(10), 981–991, doi:10.1016/S1470-2045(09)70229-3, 2009.

Chen, Z., Wei, S. and Cai, S.: [Significance and limitations of f/tPSA in differential diagnosis of prostate cancer with tPSA levels between 4 and 10 ng/ml]., Zhonghua Wai Ke Za Zhi, 42(10), 593–595, 2004.

Chevillet, J. R., Khokhlova, T. D., Giraldez, M. D., Schade, G. R., Starr, F., Wang, Y.-N., Gallichotte, E. N., Wang, K., Hwang, J. H. and Tewari, M.: Release of Cell-free MicroRNA Tumor Biomarkers into the Blood Circulation with Pulsed Focused Ultrasound: A Noninvasive, Anatomically Localized, Molecular Liquid Biopsy., Radiology, 283(1), 158–167, doi:10.1148/radiol.2016160024, 2017.

Chow, E., McLean, M., Patterson, B., Bayley, A. and Goldberg, R.: Progression of prostate cancer despite undetectable serum prostate specific antigen., Can. J. Urol., 5(4), 620–622, 1998.

D'Souza, A. L., Tseng, J. R., Pauly, K. B., Guccione, S., Rosenberg, J., Gambhir, S. S. and Glazer, G. M.: A strategy for blood biomarker amplification and localization using ultrasound., Proc. Natl.

Acad. Sci. U. S. A., 106(40), 17152–17157, doi:10.1073/pnas.0903437106, 2009.

D'Souza, A. L., Chevillet, J. R., Ghanouni, P., Yan, X., Tewari, M. and Gambhir, S. S.: Tumor characterization by ultrasound-release of multiple protein and microRNA biomarkers, preclinical and clinical evidence., PLoS One, 13(3), e0194268, doi:10.1371/journal.pone.0194268, 2018.

Dehm, S. M., Schmidt, L. J., Heemers, H. V, Vessella, R. L. and Tindall, D. J.: Splicing of a novel androgen receptor exon generates a constitutively active androgen receptor that mediates prostate cancer therapy resistance., Cancer Res., 68(13), 5469–5477, doi:10.1158/0008-5472.CAN-08-0594, 2008.

Dzinic, S. H., Bernardo, M. M., Li, X., Fernandez-Valdivia, R., Ho, Y.-S., Mi, Q.-S., Bandyopadhyay, S., Lonardo, F., Vranic, S., Oliveira, D. S. M., Bonfil, R. D., Dyson, G., Chen, K., Omerovic, A., Sheng, X., Han, X., Wu, D., Bi, X., Cabaravdic, D., Jakupovic, U., Wahba, M., Pang, A., Harajli, D., Sakr, W. A. and Sheng, S.: An Essential Role of Maspin in Embryogenesis and Tumor Suppression., Cancer Res., 77(4), 886–896, doi:10.1158/0008-5472.CAN-16-2219, 2017.

Enokida, H., Shiina, H., Urakami, S., Igawa, M., Ogishima, T., Li, L.-C., Kawahara, M., Nakagawa, M., Kane, C., Carroll, P. R. and Dahiya, R.: Multigene Methylation Analysis for Detection and Staging of Prostate Cancer, , doi:10.1158/1078-0432.CCR-05-0658, 2005.

Fan, Z., Liu, H., Mayer, M. and Deng, C. X.: Spatiotemporally controlled single cell sonoporation., Proc. Natl. Acad. Sci. U. S. A., 109(41), 16486–16491, doi:10.1073/pnas.1208198109, 2012.

Frenkel, V.: Ultrasound mediated delivery of drugs and genes to solid tumors., Adv. Drug Deliv. Rev., 60(10), 1193–1208, doi:10.1016/j.addr.2008.03.007, 2008.

Gallagher, D. J., Gaudet, M. M., Pal, P., Kirchhoff, T., Balistreri, L., Vora, K., Bhatia, J., Stadler, Z., Fine, S. W., Reuter, V., Zelefsky, M., Morris, M. J., Scher, H. I., Klein, R. J., Norton, L., Eastham, J. A., Scardino, P. T., Robson, M. E. and Offit, K.: Germline BRCA Mutations Denote a

Clinicopathologic Subset of Prostate Cancer, Diagnosis, Progn. Clin Cancer Res, 16(7), 2115–2136, doi:10.1158/1078-0432.CCR-09-2871, 2010.

Ganepola, G. A., Rutledge, J. R., Suman, P., Yiengpruksawan, A. and Chang, D. H.: Novel blood-based microRNA biomarker panel for early diagnosis of pancreatic cancer., World J. Gastrointest. Oncol., 6(1), 22–33, doi:10.4251/wjgo.v6.i1.22, 2014.

Gaspar, V. M., Correia, I. J., Sousa, A., Silva, F., Paquete, C. M., Queiroz, J. A. and Sousa, F.: Nanoparticle mediated delivery of pure P53 supercoiled plasmid DNA for gene therapy., J. Control. Release, 156(2), 212–222, doi:10.1016/j.jconrel.2011.08.007, 2011.

Georget, V., Térouanne, B., Nicolas, J.-C. and Sultan, C.: Mechanism of antiandrogen action: key role of hsp90 in conformational change and transcriptional activity of the androgen receptor., Biochemistry, 41(39), 11824–11831, doi:10.1021/bi0259150, 2002.

Giri, D., Ozen, M. and Ittmann, M.: Interleukin-6 is an autocrine growth factor in human prostate cancer., Am. J. Pathol., 159(6), 2159–2165, doi:10.1016/S0002-9440(10)63067-2, 2001.

Gleason, D. F. and Mellinger, G. T.: Prediction of Prognosis for Prostatic Adenocarcinoma by Combined Histological Grading and Clinical Staging., J. Urol., 197(2S), S134–S139, doi:10.1016/j.juro.2016.10.099, 2017.

Gorges, T. M. and Pantel, K.: Circulating tumor cells as therapy-related biomarkers in cancer patients., Cancer Immunol. Immunother., 62(5), 931–939, doi:10.1007/s00262-012-1387-1, 2013.

Hayashita, Y., Osada, H., Tatematsu, Y., Yamada, H., Yanagisawa, K., Tomida, S., Yatabe, Y., Kawahara, K., Sekido, Y. and Takahashi, T.: A polycistronic microRNA cluster, miR-17-92, is overexpressed in human lung cancers and enhances cell proliferation., Cancer Res., 65(21), 9628–9632, doi:10.1158/0008-5472.CAN-05-2352, 2005.

Hayder, H., O'Brien, J., Nadeem, U. and Peng, C.: MicroRNAs: crucial regulators of placental development., Reproduction, 155(6), R259–R271, doi:10.1530/REP-17-0603, 2018.

Hensel, K., Mienkina, M. P. and Schmitz, G.: Analysis of ultrasound fields in cell culture wells for in vitro ultrasound therapy experiments., Ultrasound Med. Biol., 37(12), 2105–2115, doi:10.1016/j.ultrasmedbio.2011.09.007, 2011.

Hernández, J., Balic, I., Johnson-Pais, T. L., Higgins, B. A., Torkko, K. C., Thompson, I. M. and Leach, R. J.: Association between an estrogen receptor alpha gene polymorphism and the risk of prostate cancer in black men., J. Urol., 175(2), 523–527, doi:10.1016/S0022-5347(05)00240-5, 2006.

Hindson, C. M., Chevillet, J. R., Briggs, H. A., Gallichotte, E. N., Ruf, I. K., Hindson, B. J., Vessella, R. L. and Tewari, M.: Absolute quantification by droplet digital PCR versus analog real-time PCR., Nat. Methods, 10(10), 1003–1005, doi:10.1038/nmeth.2633, 2013.

Horwich, A., Parker, C., de Reijke, T. and Kataja, V.: Prostate cancer: ESMO Clinical Practice Guidelines for diagnosis, treatment and follow-up., Ann. Oncol. Off. J. Eur. Soc. Med. Oncol., 24 Suppl 6, vi106-14, doi:10.1093/annonc/mdt208, 2013.

Houlgatte, A., Vincendeau, S., Desfemmes, F., Ramirez, J., Benoist, N., Bensalah, K. and Durand, X.: [Use of [-2] pro PSA and phi index for early detection of prostate cancer: a prospective of 452 patients]., Prog. en Urol. J. l'Association Fr. d'urologie la Soc. Fr. d'urologie, 22(5), 279–283, doi:10.1016/j.purol.2011.09.009, 2012.

Huber, P. E. and Pfisterer, P.: In vitro and in vivo transfection of plasmid DNA in the Dunning prostate tumor R3327-AT1 is enhanced by focused ultrasound., Gene Ther., 7(17), 1516–1525, doi:10.1038/sj.gt.3301242, 2000.

Huggins, C., Stevens, R. E. and Hodges, C. V: Studies on prostatic cancer: II. The effects of castration on advanced carcinoma of the prostate gland, Arch. Surg., 43(2), 209–223, 1941.

Humphrey, P. A.: Gleason grading and prognostic factors in carcinoma of the prostate, , doi:10.1038/modpathol.3800054, n.d.

Ilyin, S. E., Belkowski, S. M. and Plata-Salamán, C. R.: Biomarker discovery and validation: technologies and integrative approaches., Trends Biotechnol., 22(8), 411–416, doi:10.1016/j.tibtech.2004.06.005, 2004.

Ishkanian, A. S., Mallof, C. A., Ho, J., Meng, A., Albert, M., Syed, A., van der Kwast, T., Milosevic, M., Yoshimoto, M., Squire, J. A., Lam, W. L. and Bristow, R. G.: High-resolution array CGH identifies novel regions of genomic alteration in intermediate-risk prostate cancer., Prostate, 69(10), 1091–1100, doi:10.1002/pros.20959, 2009.

Izzotti, A., Carozzo, S., Pulliero, A., Zhabayeva, D., Ravetti, J. L. and Bersimbaev, R.: Extracellular MicroRNA in liquid biopsy: applicability in cancer diagnosis and prevention., Am. J. Cancer Res., 6(7), 1461–1493, 2016.

Karshafian, R., Samac, S., Bevan, P. D. and Burns, P. N.: Microbubble mediated sonoporation of cells in suspension: clonogenic viability and influence of molecular size on uptake., Ultrasonics, 50(7), 691–697, doi:10.1016/j.ultras.2010.01.009, 2010.

Kawai, N. and Iino, M.: Molecular damage to membrane proteins induced by ultrasound., Ultrasound Med. Biol., 29(4), 609–614, doi:10.1016/s0301-5629(02)00786-x, 2003.

Kelly, B. D., Miller, N., Sweeney, K. J., Durkan, G. C., Rogers, E., Walsh, K. and Kerin, M. J.: A Circulating MicroRNA Signature as a Biomarker for Prostate Cancer in a High Risk Group., J. Clin. Med., 4(7), 1369–1379, doi:10.3390/jcm4071369, 2015.

Kim, J., Roh, M. and Abdulkadir, S. A.: Pim1 promotes human prostate cancer cell tumorigenicity and c-MYC transcriptional activity., BMC Cancer, 10, 248, doi:10.1186/1471-2407-10-248, 2010.

Kishikawa, T., Otsuka, M., Ohno, M., Yoshikawa, T., Takata, A. and Koike, K.: Circulating RNAs as new biomarkers for detecting pancreatic cancer., World J. Gastroenterol., 21(28), 8527–8540, doi:10.3748/wjg.v21.i28.8527, 2015.

Knezevic, D., Goddard, A. D., Natraj, N., Cherbavaz, D. B., Clark-Langone, K. M., Snable, J.,

Watson, D., Falzarano, S. M., Magi-Galluzzi, C., Klein, E. A. and Quale, C.: Analytical validation of the Oncotype DX prostate cancer assay - a clinical RT-PCR assay optimized for prostate needle biopsies., BMC Genomics, 14, 690, doi:10.1186/1471-2164-14-690, 2013.

Knudsen, B. S. and Vasioukhin, V.: Mechanisms of prostate cancer initiation and progression., Adv. Cancer Res., 109, 1–50, doi:10.1016/B978-0-12-380890-5.00001-6, 2010.

Kristal, A. R., Price, D. K., Till, C., Schenk, J. M., Neuhouser, M. L., Ockers, S., Lin, D. W., Thompson, I. M. and Figg, W. D.: Androgen receptor CAG repeat length is not associated with the risk of incident symptomatic benign prostatic hyperplasia: results from the Prostate Cancer Prevention Trial., Prostate, 70(6), 584–590, doi:10.1002/pros.21092, 2010.

Kumar-Sinha, C., Tomlins, S. A. and Chinnaiyan, A. M.: Recurrent gene fusions in prostate cancer., Nat. Rev. Cancer, 8(7), 497–511, doi:10.1038/nrc2402, 2008.

Kumar, S., Mohan, A. and Guleria, R.: Biomarkers in cancer screening, research and detection: present and future: a review., Biomarkers Biochem. Indic. Expo. response, susceptibility to Chem., 11(5), 385–405, doi:10.1080/13547500600775011, 2006.

Lawrie, C. H., Gal, S., Dunlop, H. M., Pushkaran, B., Liggins, A. P., Pulford, K., Banham, A. H., Pezzella, F., Boultwood, J., Wainscoat, J. S., Hatton, C. S. R. and Harris, A. L.: Detection of elevated levels of tumour-associated microRNAs in serum of patients with diffuse large B-cell lymphoma, Br. J. Haematol., 141(5), 672–675, doi:10.1111/j.1365-2141.2008.07077.x, 2008.

Lawson, D. A., Zong, Y., Memarzadeh, S., Xin, L., Huang, J. and Witte, O. N.: Basal epithelial stem cells are efficient targets for prostate cancer initiation, , doi:10.1073/pnas.0913873107, n.d.

Lee, W.-H., Mortont, R. A., Epsteintt, J. I., Brookst, J. D., Campbell, P. A., Bovat, G. S., Hsieh, W.-S., Isaacs, W. B. and Nelson, W. G.: Cytidine methylation of regulatory sequences near the a-class glutathione S-transferase gene accompanies human prostatic carcinogenesis., 1994.

Lee, Y., Ahn, C., Han, J., Choi, H., Kim, J., Yim, J., Lee, J., Provost, P., Rådmark, O., Kim, S. and

Kim, V. N.: The nuclear RNase III Drosha initiates microRNA processing., Nature, 425(6956), 415–419, doi:10.1038/nature01957, 2003.

Leibovici, D., Spiess, P. E., Agarwal, P. K., Tu, S.-M., Pettaway, C. A., Hitzhusen, K., Millikan, R. E. and Pisters, L. L.: Prostate cancer progression in the presence of undetectable or low serum prostate-specific antigen level., Cancer, 109(2), 198–204, doi:10.1002/cncr.22372, 2007.

Lentacker, I., De Cock, I., Deckers, R., De Smedt, S. C. and Moonen, C. T. W.: Understanding ultrasound induced sonoporation: definitions and underlying mechanisms., Adv. Drug Deliv. Rev., 72, 49–64, doi:10.1016/j.addr.2013.11.008, 2014.

Leyten, G. H. J. M., Hessels, D., Jannink, S. A., Smit, F. P., de Jong, H., Cornel, E. B., de Reijke, T. M., Vergunst, H., Kil, P., Knipscheer, B. C., van Oort, I. M., Mulders, P. F. A., Hulsbergen-van de Kaa, C. A. and Schalken, J. A.: Prospective multicentre evaluation of PCA3 and TMPRSS2-ERG gene fusions as diagnostic and prognostic urinary biomarkers for prostate cancer., Eur. Urol., 65(3), 534–542, doi:10.1016/j.eururo.2012.11.014, 2014.

Liang, Y., Ridzon, D., Wong, L. and Chen, C.: Characterization of microRNA expression profiles in normal human tissues., BMC Genomics, 8, 166, doi:10.1186/1471-2164-8-166, 2007.

Lilja, H.: Testing new PSA subforms to enhance the accuracy of predicting cancer risk and disease outcome in prostate cancer., Clin. Chem., 54(7), 1248–1249, doi:10.1373/clinchem.2007.101204, 2008.

Lionetti, V., Fittipaldi, A., Agostini, S., Giacca, M., Recchia, F. A. and Picano, E.: Enhanced caveolae-mediated endocytosis by diagnostic ultrasound in vitro., Ultrasound Med. Biol., 35(1), 136–143, doi:10.1016/j.ultrasmedbio.2008.07.011, 2009.

Liu, H.-L., Fan, C.-H., Ting, C.-Y. and Yeh, C.-K.: Combining microbubbles and ultrasound for drug delivery to brain tumors: current progress and overview., Theranostics, 4(4), 432–444, doi:10.7150/thno.8074, 2014.

Lucchetti, D., Perelli, L., Colella, F., Ricciardi-Tenore, C., Scoarughi, G. L., Barbato, G., Boninsegna, A., De Maria, R. and Sgambato, A.: Low-intensity pulsed ultrasound affects growth, differentiation, migration, and epithelial-to-mesenchymal transition of colorectal cancer cells., J. Cell. Physiol., 235(6), 5363–5377, doi:10.1002/jcp.29423, 2020.

Luo, J., Zha, S., Gage, W. R., Dunn, T. A., Hicks, J. L., Bennett, C. J., Ewing, C. M., Platz, E. A., Ferdinandusse, S., Wanders, R. J., Trent, J. M., Isaacs, W. B. and De Marzo, A. M.: Alpha-methylacyl-CoA racemase: a new molecular marker for prostate cancer., Cancer Res., 62(8), 2220–2226, 2002.

Lv, C., Fu, S., Dong, Q., Yu, Z., Zhang, G., Kong, C., Fu, C. and Zeng, Y.: PAGE4 promotes prostate cancer cells survive under oxidative stress through modulating MAPK/JNK/ERK pathway., J. Exp. Clin. Cancer Res., 38(1), 24, doi:10.1186/s13046-019-1032-3, 2019.

Margiotti, K., Kim, E., Pearce, C. L., Spera, E., Novelli, G. and Reichardt, J. K. V: Association of the G289S single nucleotide polymorphism in the HSD17B3 gene with prostate cancer in Italian men., Prostate, 53(1), 65–68, doi:10.1002/pros.10134, 2002.

Migita, T., Ruiz, S., Fornari, A., Fiorentino, M., Priolo, C., Zadra, G., Inazuka, F., Grisanzio, C., Palescandolo, E., Shin, E., Fiore, C., Xie, W., Kung, A. L., Febbo, P. G., Subramanian, A., Mucci, L., Ma, J., Signoretti, S., Stampfer, M., Hahn, W. C., Finn, S. and Loda, M.: Fatty acid synthase: a metabolic enzyme and candidate oncogene in prostate cancer., J. Natl. Cancer Inst., 101(7), 519–532, doi:10.1093/jnci/djp030, 2009.

Mikolajczyk, S. D., Marker, K. M., Millar, L. S., Kumar, A., Saedi, M. S., Payne, J. K., Evans, C. L., Gasior, C. L., Linton, H. J., Carpenter, P. and Rittenhouse, H. G.: A truncated precursor form of prostate-specific antigen is a more specific serum marker of prostate cancer., Cancer Res., 61(18), 6958–6963, 2001.

Miller, D. L., Bao, S. and Morris, J. E.: Sonoporation of cultured cells in the rotating tube exposure

system., Ultrasound Med. Biol., 25(1), 143–149, doi:10.1016/s0301-5629(98)00137-9, 1999.

Nelson, W. G., De Marzo, A. M. and Yegnasubramanian, S.: Epigenetic alterations in human prostate cancers., Endocrinology, 150(9), 3991–4002, doi:10.1210/en.2009-0573, 2009.

Noda, D., Itoh, S., Watanabe, Y., Inamitsu, M., Dennler, S., Itoh, F., Koike, S., Danielpour, D., Ten Dijke, P. and Kato, M.: ELAC2, a putative prostate cancer susceptibility gene product, potentiates TGF-b/Smad-induced growth arrest of prostate cells, Oncogene, 25, 5591–5600, doi:10.1038/sj.onc.1209571, 2006.

Oesterling, J. E., Kumamoto, Y., Tsukamoto, T., Girman, C. J., Guess, H. A., Masumori, N., Jacobsen, S. J. and Lieber, M. M.: Serum prostate-specific antigen in a community-based population of healthy Japanese men: lower values than for similarly aged white men., Br. J. Urol., 75(3), 347–353, doi:10.1111/j.1464-410x.1995.tb07347.x, 1995.

Paproski, R. J., Forbrich, A., Hitt, M. and Zemp, R.: RNA biomarker release with ultrasound and phase-change nanodroplets, Ultrasound Med. Biol., 40(8), 1847–1856, doi:10.1016/j.ultrasmedbio.2014.01.011, 2014.

Paproski, R. J., Jovel, J., Wong, G. K.-S., Lewis, J. D. and Zemp, R. J.: Enhanced Detection of Cancer Biomarkers in Blood-Borne Extracellular Vesicles Using Nanodroplets and Focused Ultrasound., Cancer Res., 77(1), 3–13, doi:10.1158/0008-5472.CAN-15-3231, 2017.

Park, C. Y., Choi, Y. S. and McManus, M. T.: Analysis of microRNA knockouts in mice., Hum. Mol. Genet., 19(R2), R169-75, doi:10.1093/hmg/ddq367, 2010.

Pasquinelli, A. E., Reinhart, B. J., Slack, F., Martindale, M. Q., Kuroda, M. I., Maller, B., Hayward, D. C., Ball, E. E., Degnan, B., Müller, P., Spring, J., Srinivasan, A., Fishman, M., Finnerty, J., Corbo, J., Levine, M., Leahy, P., Davidson, E. and Ruvkun, G.: Conservation of the sequence and temporal expression of let-7 heterochronic regulatory RNA., Nature, 408(6808), 86–89, doi:10.1038/35040556, 2000.

Pełka, K., Klicka, K., Grzywa, T. M., Gondek, A., Marczewska, J. M., Garbicz, F., Szczepaniak, K., Paskal, W. and Włodarski, P. K.: miR-96-5p, miR-134-5p, miR-181b-5p and miR-200b-3p heterogenous expression in sites of prostate cancer versus benign prostate hyperplasia-archival samples study., Histochem. Cell Biol., 155(3), 423–433, doi:10.1007/s00418-020-01941-2, 2021.

Popa, G. T., Carol, F. " and Grozescu, T.: Prostate cancer between prognosis and adequate/proper therapy., n.d.

Porter, T. R., Iversen, P. L., Li, S. and Xie, F.: Interaction of diagnostic ultrasound with synthetic oligonucleotide-labeled perfluorocarbon-exposed sonicated dextrose albumin microbubbles., J. ultrasound Med. Off. J. Am. Inst. Ultrasound Med., 15(8), 577–584, doi:10.7863/jum.1996.15.8.577, 1996.

Porzycki, P., Ciszkowicz, E., Semik, M. and Tyrka, M.: Combination of three miRNA (miR-141, miR-21, and miR-375) as potential diagnostic tool for prostate cancer recognition., Int. Urol. Nephrol., 50(9), 1619–1626, doi:10.1007/s11255-018-1938-2, 2018.

Prensner, J. R., Rubin, M. A., Wei, J. T. and Chinnaiyan, A. M.: Beyond PSA: the next generation of prostate cancer biomarkers., Sci. Transl. Med., 4(127), 127rv3, doi:10.1126/scitranslmed.3003180, 2012.

Pritchard, C. C., Cheng, H. H. and Tewari, M.: MicroRNA profiling: approaches and considerations., Nat. Rev. Genet., 13(5), 358–369, doi:10.1038/nrg3198, 2012.

Punnoose, E. A., Atwal, S. K., Spoerke, J. M., Savage, H., Pandita, A., Yeh, R.-F., Pirzkall, A., Fine, B. M., Amler, L. C., Chen, D. S. and Lackner, M. R.: Molecular biomarker analyses using circulating tumor cells., PLoS One, 5(9), e12517, doi:10.1371/journal.pone.0012517, 2010.

Reid, A. H. M., Attard, G., Ambroisine, L., Fisher, G., Kovacs, G., Brewer, D., Clark, J., Flohr, P., Edwards, S., Berney, D. M., Foster, C. S., Fletcher, A., Gerald, W. L., Møller, H., Reuter, V. E., Scardino, P. T., Cuzick, J., de Bono, J. S. and Cooper, C. S.: Molecular characterisation of ERG,

ETV1 and PTEN gene loci identifies patients at low and high risk of death from prostate cancer., Br. J. Cancer, 102(4), 678–684, doi:10.1038/sj.bjc.6605554, 2010.

Rodriguez, A., Griffiths-Jones, S., Ashurst, J. L. and Bradley, A.: Identification of mammalian microRNA host genes and transcription units., Genome Res., 14(10A), 1902–1910, doi:10.1101/gr.2722704, 2004.

Romero Otero, J., Garcia Gomez, B., Campos Juanatey, F. and Touijer, K. A.: Prostate cancer biomarkers: an update., Urol. Oncol., 32(3), 252–260, doi:10.1016/j.urolonc.2013.09.017, 2014.

Ruivo, C. F., Arbara Adem, B., Silva, M., Onia, S. and Melo, A.: The Biology of Cancer Exosomes: Insights and New Perspectives, , doi:10.1158/0008-5472.CAN-17-0994, 2017.

Russo, F., Di Bella, S., Vannini, F., Berti, G., Scoyni, F., Cook, H. V, Santos, A., Nigita, G., Bonnici, V., Laganà, A., Laganà, L., Geraci, F., Pulvirenti, A., Giugno, R., De Masi, F., Belling, K., Jensen, L. J., Brunak, S., Pellegrini, M. and Ferro, A.: miRandola 2017: a curated knowledge base of non-invasive biomarkers, Nucleic Acids Res., 46, doi:10.1093/nar/gkx854, 2018.

Rybak, A. P., Bristow, R. G. and Kapoor, A.: Prostate cancer stem cells: deciphering the origins and pathways involved in prostate tumorigenesis and aggression., Oncotarget, 6(4), 1900–1919, doi:10.18632/oncotarget.2953, 2015.

Sager, R., Sheng, S., Pemberton, P. and Hendrix, M. J.: Maspin: a tumor suppressing serpin., Curr. Top. Microbiol. Immunol., 213 (Pt 1, 51–64, doi:10.1007/978-3-642-61107-0_4, 1996.

Saini, S.: PSA and beyond: alternative prostate cancer biomarkers., Cell. Oncol. (Dordr)., 39(2), 97–106, doi:10.1007/s13402-016-0268-6, 2016.

Sarma, A. V, Dunn, R. L., Lange, L. A., Ray, A., Wang, Y., Lange, E. M. and Cooney, K. A.: Genetic polymorphisms in CYP17, CYP3A4, CYP19A1, SRD5A2, IGF-1, and IGFBP-3 and prostate cancer risk in African-American men: the Flint Men's Health Study., Prostate, 68(3), 296–305, doi:10.1002/pros.20696, 2008.

Sartori, D. A. and Chan, D. W.: Biomarkers in prostate cancer: what's new?, Curr. Opin. Oncol., 26(3), 259–264, doi:10.1097/CCO.0000000000000065, 2014.

Sato, H., Minei, S., Hachiya, T., Yoshida, T. and Takimoto, Y.: Fluorescence in situ hybridization analysis of c-myc amplification in stage TNM prostate cancer in Japanese patients., Int. J. Urol. Off. J. Japanese Urol. Assoc., 13(6), 761–766, doi:10.1111/j.1442-2042.2006.01399.x, 2006.

Sboros, V.: Response of contrast agents to ultrasound., Adv. Drug Deliv. Rev., 60(10), 1117–1136, doi:10.1016/j.addr.2008.03.011, 2008.

Schoenborn, J. R., Nelson, P. and Fang, M.: Genomic profiling defines subtypes of prostate cancer with the potential for therapeutic stratification., Clin. cancer Res. an Off. J. Am. Assoc. Cancer Res., 19(15), 4058–4066, doi:10.1158/1078-0432.CCR-12-3606, 2013.

Seruga, B., Ocana, A. and Tannock, I. F.: Drug resistance in metastatic castration-resistant prostate cancer, Nat. Rev. Clin. Oncol., 8(1), 12–23, doi:10.1038/nrclinonc.2010.136, 2011.

Shen, M. M. and Abate-Shen, C.: Pten inactivation and the emergence of androgen-independent prostate cancer., Cancer Res., 67(14), 6535–6538, doi:10.1158/0008-5472.CAN-07-1271, 2007.

Suzuki, M., Muto, S., Hara, K., Ozeki, T., Yamada, Y., Kadowaki, T., Tomita, K., Kameyama, S. and Kitamura, T.: Single-nucleotide polymorphisms in the 17beta-hydroxysteroid dehydrogenase genes might predict the risk of side-effects of estramustine phosphate sodium in prostate cancer patients., Int. J. Urol. Off. J. Japanese Urol. Assoc., 12(2), 166–172, doi:10.1111/j.1442-2042.2005.01004.x, 2005.

Tagawa, H. and Seto, M.: A microRNA cluster as a target of genomic amplification in malignant lymphoma., Leukemia, 19(11), 2013–2016, doi:10.1038/sj.leu.2403942, 2005.

Tomlins, S. A., Rhodes, D. R., Yu, J., Varambally, S., Mehra, R., Perner, S., Demichelis, F., Helgeson, B. E., Laxman, B., Morris, D. S., Cao, Q., Cao, X., Andrén, O., Fall, K., Johnson, L., Wei, J. T., Shah, R. B., Al-Ahmadie, H., Eastham, J. A., Eggener, S. E., Fine, S. W., Hotakainen,

K., Stenman, U.-H., Tsodikov, A., Gerald, W. L., Lilja, H., Reuter, V. E., Kantoff, P. W., Scardino, P. T., Rubin, M. A., Bjartell, A. S. and Chinnaiyan, A. M.: The role of SPINK1 in ETS rearrangement-negative prostate cancers., Cancer Cell, 13(6), 519–528, doi:10.1016/j.ccr.2008.04.016, 2008.

Turchinovich, A., Weiz, L., Langheinz, A. and Burwinkel, B.: Characterization of extracellular circulating microRNA., Nucleic Acids Res., 39(16), 7223–7233, doi:10.1093/nar/gkr254, 2011.

Unger, E. C., Hersh, E., Vannan, M. and McCreery, T.: Gene delivery using ultrasound contrast agents., Echocardiography, 18(4), 355–361, doi:10.1046/j.1540-8175.2001.00355.x, 2001.

Urabe, F., Matsuzaki, J., Yamamoto, Y., Kimura, T., Hara, T., Ichikawa, M., Takizawa, S., Aoki, Y., Niida, S., Sakamoto, H., Kato, K., Egawa, S., Fujimoto, H. and Ochiya, T.: Large-scale Circulating microRNA Profiling for the Liquid Biopsy of Prostate Cancer., Clin. cancer Res. an Off. J. Am. Assoc. Cancer Res., 25(10), 3016–3025, doi:10.1158/1078-0432.CCR-18-2849, 2019.

Urisman, A., Molinaro, R. J., Fischer, N., Plummer, S. J., Casey, G., Klein, E. A., Malathi, K., Magi-Galluzzi, C., Tubbs, R. R., Ganem, D., Silverman, R. H. and DeRisi, J. L.: Retraction. Identification of a novel gammaretrovirus in prostate tumors of patients homozygous for R462Q RNASEL variant., PLoS Pathog., 8(9), doi:10.1371/annotation/7e2efc01-2e9b-4e9b-aef0-87ab0e4e4732, 2012.

VanBavel, E.: Effects of shear stress on endothelial cells: possible relevance for ultrasound applications., Prog. Biophys. Mol. Biol., 93(1–3), 374–383, doi:10.1016/j.pbiomolbio.2006.07.017, 2007.

Varambally, S., Dhanasekaran, S. M., Zhou, M., Barrette, T. R., Kumar-Sinha, C., Sanda, M. G., Ghosh, D., Pienta, K. J., Sewalt, R. G. A. B., Otte, A. P., Rubin, M. A. and Chinnaiyan, A. M.: The polycomb group protein EZH2 is involved in progression of prostate cancer., Nature, 419(6907), 624–629, doi:10.1038/nature01075, 2002.

Vlaeminck-Guillem, V., Ruffion, A., André, J., Devonec, M. and Paparel, P.: Urinary prostate cancer 3 test: toward the age of reason?, Urology, 75(2), 447–453, doi:10.1016/j.urology.2009.03.046, 2010.

Wang, J., Cai, Y., Yu, W., Ren, C., Spencer, D. M. and Ittmann, M.: Pleiotropic Biological Activities of Alternatively Spliced TMPRSS2/ERG Fusion Gene Transcripts, Cancer Res, doi:10.1158/0008-5472.CAN-08-1147, 2008.

Wang, L., Liu, R., Li, W., Chen, C., Katoh, H., Chen, G.-Y., McNally, B., Lin, L., Zhou, P., Zuo, T., Cooney, K. A., Liu, Y. and Zheng, P.: Somatic single hits inactivate the X-linked tumor suppressor FOXP3 in the prostate., Cancer Cell, 16(4), 336–346, doi:10.1016/j.ccr.2009.08.016, 2009.

Wang, Y. and Yuan, F.: Delivery of viral vectors to tumor cells: extracellular transport, systemic distribution, and strategies for improvement., Ann. Biomed. Eng., 34(1), 114–127, doi:10.1007/s10439-005-9007-2, 2006.

Wang, Y., Medvid, R., Melton, C., Jaenisch, R. and Blelloch, R.: DGCR8 is essential for microRNA biogenesis and silencing of embryonic stem cell self-renewal., Nat. Genet., 39(3), 380–385, doi:10.1038/ng1969, 2007.

Witwer, K. W.: Circulating microRNA biomarker studies: pitfalls and potential solutions., Clin. Chem., 61(1), 56–63, doi:10.1373/clinchem.2014.221341, 2015.

Won, Y.-W., Kim, K.-M., An, S. S., Lee, M., Ha, Y. and Kim, Y.-H.: Suicide gene therapy using reducible poly (oligo-D-arginine) for the treatment of spinal cord tumors., Biomaterials, 32(36), 9766–9775, doi:10.1016/j.biomaterials.2011.08.089, 2011.

Xing, Y., Lu, X., Pua, E. C. and Zhong, P.: The effect of high intensity focused ultrasound treatment on metastases in a murine melanoma model, Biochem. Biophys. Res. Commun., 375(4), 645–650, doi:10.1016/j.bbrc.2008.08.072, 2008.

Xu, J., Meyers, D., Freije, D., Isaacs, S., Wiley, K., Nusskern, D., Ewing, C., Wilkens, E., Bujnovszky, P., Bova, G. S., Walsh, P., Isaacs, W., Schleutker, J., Matikainen, M., Tammela, T., Visakorpi, T., Kallioniemi, O. P., Berry, R., Schaid, D., French, A., McDonnell, S., Schroeder, J., Blute, M., Thibodeau, S., Grönberg, H., Emanuelsson, M., Damber, J. E., Bergh, A., Jonsson, B. A., Smith, J., Bailey-Wilson, J., Carpten, J., Stephan, D., Gillanders, E., Amundson, I., Kainu, T., Freas-Lutz, D., Baffoe-Bonnie, A., Van Aucken, A., Sood, R., Collins, F., Brownstein, M. and Trent, J.: Evidence for a prostate cancer susceptibility locus on the X chromosome., Nat. Genet., 20(2), 175–179, doi:10.1038/2477, 1998.

Xu, W., San Lucas, A., Wang, Z. and Liu, Y.: Identifying microRNA targets in different gene regions., BMC Bioinformatics, 15 Suppl 7(Suppl 7), S4, doi:10.1186/1471-2105-15-S7-S4, 2014.

Yang, W. J., Yang, D. D., Na, S., Sandusky, G. E., Zhang, Q. and Zhao, G.: Dicer Is Required for Embryonic Angiogenesis during Mouse Development*, , doi:10.1074/jbc.M413394200, 2004.

Zhang, Y.-A., Nemunaitis, J., Samuel, S. K., Chen, P., Shen, Y. and Tong, A. W.: Antitumor activity of an oncolytic adenovirus-delivered oncogene small interfering RNA., Cancer Res., 66(19), 9736–9743, doi:10.1158/0008-5472.CAN-06-1617, 2006.

Zhou, Y., Kumon, R. E., Cui, J. and Deng, C. X.: The size of sonoporation pores on the cell membrane., Ultrasound Med. Biol., 35(10), 1756–1760, doi:10.1016/j.ultrasmedbio.2009.05.012, 2009.

Zhu, S., Lee, D. A. and Li, S.: IL-12 and IL-27 sequential gene therapy via intramuscular electroporation delivery for eliminating distal aggressive tumors., J. Immunol., 184(5), 2348–2354, doi:10.4049/jimmunol.0902371, 2010.

ACKNOWLEDGEMENTS

Ringrazio tutti coloro che hanno reso possibile questo progetto: in primis, la Professoressa Francesca Zazzeroni che mi ha dato l'opportunità di entrare a far parte del suo team e senza la cui guida non avrei potuto sviluppare questo lavoro; il Dottor Barbato, rappresentate della partnership industriale PON fondamentale per il mio approccio tecnico allo strumento; la Professoressa Alessandra Tessitore e la Professoressa Monica di Padova che hanno sostenuto la parte sperimentale del progetto con le loro expertise; la dottoressa Daria Capece che mi supportato durante tutta la stesura di questa tesi e, ovviamente, il Rettore Alesse, mentore del nostro laboratorio.

Un sentito grazie a tutto il team del laboratorio Zazzeroni-Tessitore: Barbara, Mauro, Irene, Daniela, Davide, Chiara, Roberta e Alessandra, compagni di viaggio unici che mi hanno consigliata, sostenuta e hanno reso la mia esperienza non solo formativa a livello accademico ma anche a livello umano.

Grazie di cuore alla mia famiglia, senza il cui sostegno tutto il mio percorso sarebbe stato impossibile.

La borsa di dottorato è stata cofinanziata con risorse del Programma Operativo Nazionale 2014-2020 (CCI 2014IT16M2OP005), Fondo Sociale Europeo, Azione I.1 “Dottorati Innovativi con caratterizzazione industriale”